


FineVLA: Fine-Grained Instruction Alignment for Steerable Vision-Language-Action Policies

Xintong Hu^{*x} Xuhong Huang^{*x} Jinyu Zhang^x Yutong Yao^x Yuchong Sun^q
 Qiuyue Wang^q Mingsheng Li^q Sicheng Xie^q Yitao Liu^x Junhao Chen^x
 Yixuan Chen^x Yingming Zheng^x Shuai Bai^q Tao Yu^{†x}

^x XLANG Lab, The University of Hong Kong ^q Qwen Team, Alibaba Inc.

 FineVLA Project Page: <https://finevla.xlang.ai/>

Abstract

Vision-Language-Action (VLA) models are increasingly expected to not only complete robot tasks, but also follow human instructions about *how* those tasks should be executed. However, existing robot datasets usually pair trajectories with coarse goal-level language, leaving execution-critical details such as active arm, approach direction, and contact region unspecified. This limits steerable policy learning and robotic video understanding. We introduce **FineVLA**, an open framework for action-aligned fine-grained VLA supervision. The framework includes: (1) a data construction tool that unifies 972,247 trajectories across 85K tasks from 10 open-source robot datasets and builds **FineVLA-Data**, a human-verified dataset of 47,159 fine-grained trajectories; (2) a held-out benchmark with 500 videos, 10,816 atomic facts, and 1,030 VQA questions; (3) a robotics-specialized VLM annotator for scalable fine-grained annotation; and (4) a steerable **VLA policy** trained with controlled mixtures of fine-grained and raw goal-level instructions. Our policy experiments yield three findings. First, fine-grained supervision does not sacrifice goal-level task success: fine-grained-only (FG-only) improves over raw-instruction-only (Raw-only) by +1.4 to +8.1 success-rate points across architecture and data-scale settings. Second, fine-grained and raw instructions are complementary: performance follows a consistent inverted-U trend, peaking around FG : Raw = 1 : 2 to 1 : 1. The strongest mixed setting reaches **86.8%/82.5%** in RoboTwin simulation and **62.7/100** in real-world dual-arm manipulation, compared with 49.9 for Raw-only. Third, fine-grained supervision directly improves steerable control by increasing compliance with language-specified execution factors: in real-world evaluation, the largest gains over Raw-only appear on pose (+23), color (+18), and approach direction (+18)—factors where goal-level instructions provide no guidance. Overall, fine-grained language should augment goal-level instructions: specifying *how* to execute alongside *what* to achieve.

1 Introduction

Vision-Language-Action (VLA) models are moving from task-level robot control toward policies that can be *steered* by human instructions. In this work, we use *steerability* to mean the ability to execute the same high-level goal in different ways according to user-specified execution constraints, such as which arm to use, which target object to manipulate, how to approach it, where to make contact,

* Equal contribution. † Corresponding authors.

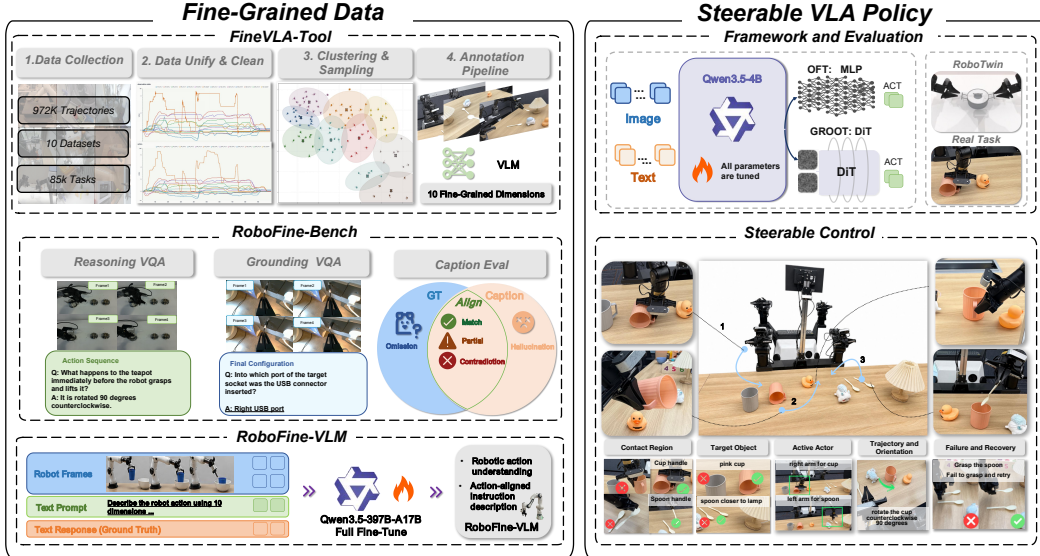


Figure 1: **Overview of FineVLA.** FineVLA builds a closed loop for action-instruction alignment, connecting fine-grained data construction, robotic video understanding, scalable annotation, and steerable VLA policy learning. **Left:** FineVLA-Tool unifies heterogeneous robot trajectories from 10 open-source datasets, removes redundant demonstrations through clustering and sampling, and annotates representative trajectories with action-aligned descriptions across ten fine-grained dimensions. The resulting FineVLA-Data supports both RoboFine-Bench, which evaluates fine-grained robotic video understanding through Grounding VQA, Reasoning VQA, and Caption Evaluation, and RoboFine-VLM, a robotics-specialized VLM trained as a scalable annotator for new trajectories. **Right:** FineVLA-Policy is trained with mixtures of raw goal-level instructions and fine-grained process-level instructions under two action-decoding architectures, and is evaluated in both RoboTwin simulation and real-world dual-arm manipulation. The steerable-control examples illustrate how fine-grained language specifies execution-sensitive factors such as contact region, target object, active actor, trajectory and orientation, and failure recovery.

which motion or rotation direction to follow, and what final configuration to achieve. Recent robot foundation models such as $\pi_{0.7}$, LingBot-VLA, GROOT N1.7, and GEN-1 (1, 2, 3, 4) suggest that future robot policies should not only infer *what* task to complete, but also follow instructions about *how* the task should be performed.

However, building open, steerable VLA systems remains challenging for three reasons. **(i) Heterogeneous data and missing fine-grained annotation infrastructure.** Existing open-source robot datasets use diverse action and state representations that cannot be directly unified (5, 6). Within the same task, demonstrations are heavily redundant, and most trajectories carry only a single goal-level description (e.g., “pick up the cup”) while the execution process—actor choice, approach direction, contact region, motion path, and state transitions—remains unspecified. The problem is not only that labels are coarse, but that there is still no open infrastructure for producing action-aligned fine-grained supervision at scale. **(ii) Lack of benchmarks and scalable annotators for fine-grained robotic video understanding.** Although general video-language models and dense captioning methods have advanced video description, their captions often focus on scene appearance rather than action-relevant execution details such as contact regions, approach directions, and motion paths. Existing embodied benchmarks (7, 8, 9) mainly evaluate spatial reasoning or hand-object dynamics, but do not systematically measure whether VLMs capture process-level manipulation details. There is also a lack of open, robotics-specialized annotators for action-aligned fine-grained captions. **(iii) Unknown effectiveness and training recipe.** Even if fine-grained data were available, the community lacks systematic evidence on whether action-aligned instructions improve policy learning, and what mixture of fine-grained and goal-level supervision yields the best steerable control.

To address these challenges, we introduce **FineVLA**, a fully open-source framework for scaling fine-grained VLA data, robotic video understanding, and steerable VLA policies (Figure 1). The framework operationalizes this principle through four components, each targeting one of the gaps

above. **(1) FineVLA-Tool + FineVLA-Data (Gap i).** FineVLA-Tool unifies 972,247 trajectories across 85K tasks from 10 open-source datasets, selects representative samples via dynamic time warping (DTW)-based clustering, and annotates them with process-level descriptions across ten fine-grained dimensions (Table 9). This produces **FineVLA-Data**, a human-verified corpus of 47,159 trajectories whose average instruction length increases $10.4\times$ (from 9.3 to 96.8 words). **(2) RoboFine-Bench (Gap ii).** We curate RoboFine-Bench—500 videos with 10,816 human-reviewed atomic facts and 1,030 VQA questions spanning all ten fine-grained dimensions, with complementary VQA and caption tracks. All benchmark trajectories are held out from both VLM fine-tuning and policy training, ensuring an independent evaluation. **(3) RoboFine-VLM (Gap ii).** We fine-tune Qwen3.5-397B-A17B (10) on FineVLA-Data to obtain RoboFine-VLM, a VLM specialized for robotic action understanding that serves as a scalable annotator for new trajectories. **(4) FineVLA-Policy + training recipe (Gap iii).** We train FineVLA-Policy under two action-decoding architectures (StarVLA-OFT and StarVLA-GR00T) and systematically vary the ratio between fine-grained (FG) and raw goal-level (Raw) instructions—keeping trajectories, actions, and visual observations fixed while changing only the paired language—to isolate the effect of action-aligned supervision.

Our policy experiments yield three key findings. First, fine-grained supervision does not harm goal-level task success; instead, FG-only outperforms Raw-only across the evaluated simulation settings, with the largest gain on AlohaMix-OFT (+6.5/+4.7 points on Easy/Hard). Second, fine-grained and raw instructions are complementary: success follows an inverted-U trend over the FG:Raw ratio and peaks around 1:2–1:1, reaching **86.8%/82.5%** on AlohaMix-OFT Easy/Hard (+15.0/+11.1 over the Raw-only baseline of 71.8%/71.4%). Third, in real-world dual-arm manipulation, the FG:Raw = 1:1 policy achieves the highest average score (**62.7/100** vs. 49.9 for Raw-only), with the largest per-factor gains on execution-sensitive attributes such as pose (+23), color (+18), and approach direction (+18). Under identical visual scenes, varying only the fine-grained instruction produces distinctly different execution behaviors, directly demonstrating steerable control. In addition, RoboFine-VLM achieves the best performance among evaluated VLMs on the held-out RoboFine-Bench, reaching **71.0%** VQA accuracy and **83.6%** captioning score under the hard setting, providing evidence that our annotation schema captures action-relevant manipulation details. We release the complete FineVLA suite—data pipeline, fine-grained annotations, benchmark, model checkpoints, and training code—to provide open foundations for steerable VLA research.

2 FineVLA Data: Construction, Benchmark, and Scalable Annotation

This section describes the data and annotation substrate of FineVLA. We first unify heterogeneous robot demonstrations and construct human-verified fine-grained action-aligned instructions. We then build a held-out benchmark to evaluate process-level robotic video understanding, and finally instantiate RoboFine-VLM as a scalable annotator for extending the same annotation schema to new trajectories.

FineVLA-Tool converts large-scale heterogeneous robot datasets into fine-grained, action-aligned instruction supervision (Figure 2). Its design addresses three practical bottlenecks in open robot data: (1) inconsistent action/state formats across datasets, (2) heavy redundancy among demonstrations of the same task, and (3) sparse, task-level instruction annotations. Starting from 972,247 trajectories across 10 source datasets, FineVLA-Tool produces FineVLA-Data, a human-verified corpus of 47,159 representative trajectories with fine-grained process-level supervision.

2.1 FineVLA-Tool: Canonicalization, Clustering, and Annotation

Data collection and format conversion (Figure 2, Stage 1). We aggregate 972,247 trajectories from 10 open-source datasets (11, 12, 13, 14, 15, 16, 17, 18, 6, 19), convert them to the LeRobot 2.1 format, and filter out invalid or degenerate recordings. The full per-dataset breakdown is in Appendix A.1.1.

Action-state canonicalization and cleaning (Figure 2, Stage 2). Across datasets, action and state values differ in temporal reference (absolute, relative, or delta) and kinematic representation (joint space vs. end-effector space with varied rotation encodings). We canonicalize all trajectories to absolute coordinates with normalized quaternion rotations, then remove trajectories whose action-state DTW distance exceeds a dataset-specific threshold, filtering out corrupted logs or inconsistent control conventions. Details and conversion examples are in Appendix A.1.2.

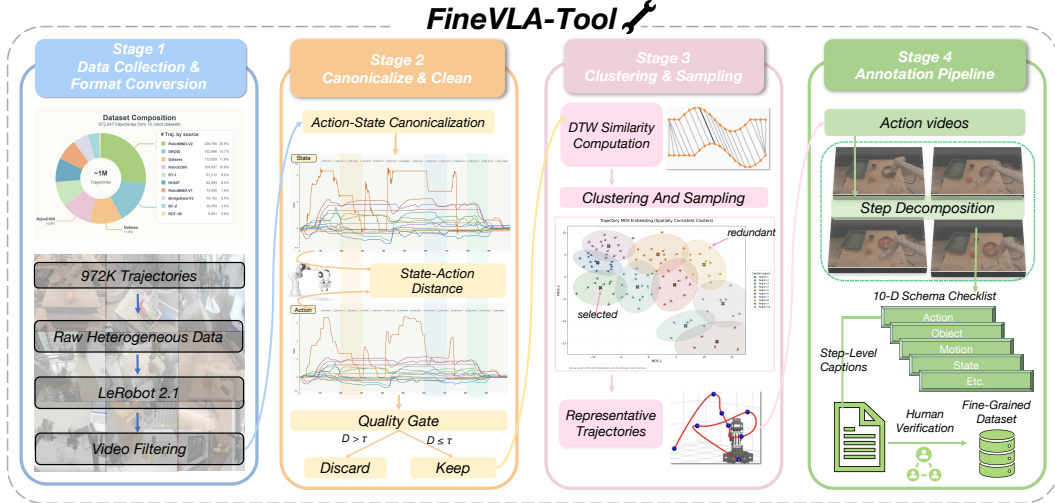


Figure 2: **Pipeline of FineVLA-Tool.** FineVLA-Tool converts large-scale heterogeneous robot demonstrations into action-aligned fine-grained instruction data through four stages. **Stage 1:** raw trajectories from 10 open-source robot datasets are converted into a unified LeRobot-style format and filtered to remove invalid videos. **Stage 2:** action and state representations are canonicalized across embodiments, and an action-state consistency quality gate removes corrupted or inconsistent trajectories. **Stage 3:** dynamic time warping (DTW)-based similarity computation and clustering identify representative trajectories, reducing redundancy while preserving diverse manipulation strategies. **Stage 4:** selected trajectories are decomposed into step-level descriptions and annotated with a ten-dimensional fine-grained schema, followed by human verification. The resulting FineVLA-Data provides human-verified, process-level supervision for training RoboFine-VLM as a scalable annotator and FineVLA-Policy as a steerable VLA policy.

Trajectory clustering and representative sampling (Figure 2, Stage 3). Open robot datasets contain many near-duplicate demonstrations within the same task, often differing only in execution speed or minor spatial offsets. To maximize annotation diversity under a fixed budget, we cluster trajectories within each task using DTW over canonicalized action sequences, followed by hierarchical clustering on the resulting distance matrix. We then select high-quality representatives from each cluster according to cluster size and trajectory quality. This reduces 972,247 raw trajectories to 47,159 representative samples while preserving diversity in manipulation strategies, object interactions, and motion patterns. Details of the DTW formulation, action-space normalization, frame costs, and clustering procedure are provided in Appendix A.1.4.

Fine-grained multi-aspect annotation (Figure 2, Stage 4). Each selected trajectory is annotated with a ten-dimensional schema capturing the control-relevant factors that goal-level instructions omit: *action sequence*, *active actor*, *target object*, *initial configuration*, *final configuration*, *contact and approach*, *trajectory and orientation*, *object interaction*, *failure and recovery*, and *body motion*. Detailed definitions and examples are provided in Appendix A.1.5, Table 9. Annotation proceeds in two phases: we first input sampled video frames from each trajectory into Qwen3.5-Plus (10), which decomposes the manipulation process into temporally ordered steps and fills structured slots for actor, target, contact region, motion path, and state change; human annotators then review the model-generated descriptions against the original video, correcting factual errors and verifying temporal alignment. The result is FineVLA-Data, a human-verified fine-grained instruction dataset for training RoboFine-VLM and downstream controllable VLA policies.

2.2 FineVLA-Data Statistics

Table 1 summarizes the statistics of FineVLA-Data. Fine-grained annotations dramatically increase instruction information density compared to original coarse instructions: the average word count per trajectory rises from 9.3 to 96.8, an approximately $10.4\times$ increase, while covering 47 unique action verbs across all sources. Detailed source dataset statistics are reported in Appendix A.1.1, Table 6.

Table 1: **FineVLA-Data statistics.** Fine-grained annotations dramatically increase instruction information density compared to original coarse instructions across all data sources.

Source	Trajectories	Steps	Avg. Words (Coarse)	Avg. Words (FG)	Density \uparrow
BridgeData-V2	4,958	21,554	10.1	61.7	6.1 \times
BC-Z	1,513	5,313	5.2	51.2	9.8 \times
RT-1	5,232	22,023	6.8	61.4	9.1 \times
Galaxea	2,834	18,484	4.7	219.9	47.1 \times
RoboMIND-V1	4,605	20,341	8.6	72.8	8.5 \times
RoboMIND-V2	7,119	39,166	6.6	98.8	14.9 \times
RoboCOIN	8,513	43,926	16.1	122.6	7.6 \times
RH20T	1,387	5,560	7.9	92.1	11.7 \times
RDT	1,275	8,437	16.9	114.0	6.7 \times
DROID	9,723	35,802	8.0	90.9	11.3 \times
Total	47,159	220,606	9.3	96.8	10.4 \times

2.3 RoboFine-Bench: Fine-Grained Robotic Video Understanding Benchmark

We introduce RoboFine-Bench to evaluate whether VLMs capture execution-level details of robot manipulation. The benchmark contains 500 videos from 10 robot datasets, covering 32 embodiments, diverse camera views, and a wide range of manipulation tasks. Each trajectory is paired with human-reviewed step-level annotations decomposed into 10,816 atomic facts across ten action-relevant dimensions (Table 9), with an average of 4.3 steps and 21.6 facts per sample. All 500 benchmark trajectories are strictly disjoint from both the RoboFine-VLM SFT training set and all policy-training splits—no trajectory appears in both the 47,159 training samples and the benchmark. Figure 3 illustrates the benchmark statistics and structure.

RoboFine-Bench contains two complementary tracks. The **VQA track** (Figure 3, right bottom) evaluates discriminative understanding through 1,030 questions distributed across the same ten fine-grained dimensions used in annotation, which are aggregated into three reporting axes: **Entity and Scene Grounding**, **Action and Motion Understanding**, and **Interaction and State Reasoning** (Table 16 in Appendix A.3.2). Each model receives video frames and all questions for one sample in a single prompt, and answers are scored by deterministic matching against ground-truth labels. The **Caption track** (Figure 3, right top) evaluates generative understanding by asking models to produce action-aligned step-level fine-grained descriptions of the manipulation process. Generated captions are then judged by an LLM against pre-extracted ground-truth atomic facts, yielding perfect alignment labels (match, partial, contradiction, omission, hallucination) that are aggregated into Consistency, Coverage, and Anti-Hallucination metrics. Two settings are evaluated: *easy*, where the original task instruction is provided, and *hard*, where the model must infer the process from visual observations alone. Full prompt templates and the evaluation protocol are provided in Appendix A.3.4.

2.4 RoboFine-VLM: Scalable Fine-Grained Annotator

While FineVLA-Data is human verified, scaling the same annotation schema to future robot trajectories still requires a robotics-specialized annotator. General-purpose VLMs often miss execution-level details such as contact regions, approach directions, grasp types, motion paths, and object state transitions, leading to substantial human correction cost.

We therefore fine-tune Qwen3.5-397B-A17B (10) on the human-verified FineVLA-Data to obtain RoboFine-VLM. Given a robot manipulation video, RoboFine-VLM generates temporally action-aligned step-level fine-grained descriptions covering the ten fine-grained dimensions (Table 9). The model serves as a scalable annotator for future data expansion; all policy experiments in this paper use FineVLA-Tool-generated and human-verified annotations, rather than RoboFine-VLM-generated labels. Importantly, RoboFine-VLM is not used to generate the supervision for our policy experiments; it is trained to support future scalable annotation and open-source reproducibility. Full training details are provided in Appendix A.2.2; its annotation quality is evaluated on the held-out RoboFine-Bench in Section 4.2.

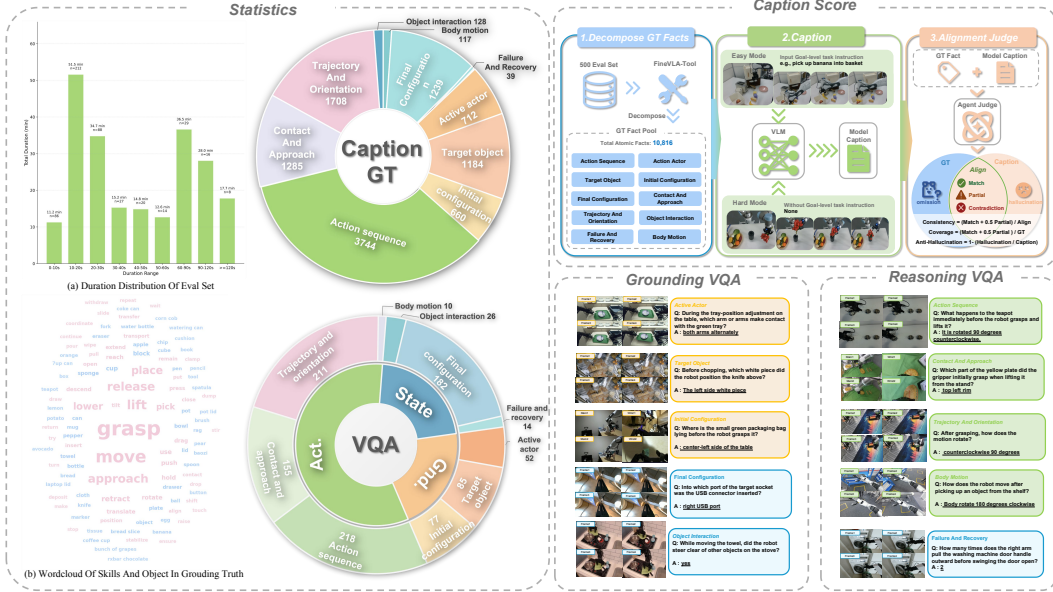


Figure 3: **Overview of RoboFine-Bench.** RoboFine-Bench evaluates fine-grained robotic video understanding through complementary VQA and captioning tracks. **Left:** benchmark statistics, including the video-duration distribution, the word cloud of manipulation skills and objects, and the distribution of ground-truth atomic facts across the ten FineVLA dimensions for captioning and VQA. **Top right:** the captioning track decomposes human-reviewed annotations into a pool of 10,816 atomic facts, asks VLMs to generate ordered step-level action descriptions under easy and hard settings, and uses an LLM judge to align model captions with ground-truth facts, producing Consistency, Coverage, and Anti-Hallucination scores. **Bottom right:** representative Grounding VQA and Reasoning VQA examples probe object/scene grounding, action/motion understanding, and interaction/state reasoning. RoboFine-Bench contains 500 held-out robot videos and 1,030 VQA questions across diverse embodiments, camera views, and manipulation scenarios.

3 Training Fine-Grained VLA Policies

With human-verified fine-grained instructions fixed, we now study how they should be used to train steerable VLA policies. Our goal is not to propose a new policy architecture, but to isolate the effect of action-aligned language supervision. We therefore keep actions, and visual observations fixed, and vary only the instruction paired with each trajectory.

3.1 FineVLA-Policy Architecture

We instantiate FineVLA-Policy under multiple action-decoding frameworks to isolate the effect of instruction supervision from architectural choices. Rather than proposing a new architecture, we adopt two existing frameworks implemented in the StarVLA codebase (20), both built on a shared Qwen3.5-4B vision-language backbone.

StarVLA-OFT attaches a lightweight MLP regression head that reads the hidden states of predefined action tokens and predicts continuous action chunks in parallel with an L1 objective, following OpenVLA-OFT. **StarVLA-GR00T** adopts a dual-system design where the VL backbone serves as System 2 for slow reasoning and a DiT-based flow-matching module serves as System 1 for continuous action generation, consistent with GR00T N1.5. Both variants produce multi-step action chunks and share the same visual observations and language inputs; only the action decoding differs. Using two architectures lets us verify that the benefits of fine-grained supervision are architecture-independent.

3.2 Training Data Mixtures

To isolate the effect of language supervision, we construct two parallel training datasets from the same source trajectories. The **FG dataset** contains the representative trajectories selected by FineVLA-Tool, each paired with its fine-grained process-level instruction (1,287 trajectories for RDT; 5,872 for

AlohaMix). The **Raw dataset** contains *all* source trajectories, each paired with its original goal-level instruction (6,061 for RDT; 84,067 for AlohaMix). AlohaMix is an ALOHA-compatible dual-arm mixture aggregated from RDT, RoboCOIN, RoboMIND-V1.0, and RoboMIND-V2.0, containing 86,662 episodes across 598 tasks (Table 21 in Appendix A.4.2). We restrict the mixture to a single embodiment class to avoid cross-embodiment confounds. Trajectories that appear in both datasets share identical action labels and visual observations; only the paired language instruction differs.

The FG:Raw ratio controls the probability of drawing from each dataset at every training step, and therefore determines the relative number of training iterations that use fine-grained versus raw instructions. For example, FG:Raw = 2:1 means the FG dataset is sampled with twice the weight of the Raw dataset, so approximately two-thirds of training steps use a fine-grained instruction and one-third use a raw instruction. Under Raw-only, training draws exclusively from the Raw dataset; under FG-only, exclusively from the FG dataset.

We compare seven configurations: Raw-only, FG:Raw = 1:4, 1:2, 1:1, 2:1, 4:1, and FG-only. We study three (dataset, framework) combinations—RDT-OFT, RDT-GR00T, and AlohaMix-OFT—to control for architecture and data-scale effects. This design isolates the effect of action-aligned language supervision from changes in data scale, embodiment, or action distribution.

4 Experiments

We evaluate FineVLA along three axes: (1) whether RoboFine-VLM captures fine-grained robotic action details (RoboFine-Bench, Section 4.2), (2) whether fine-grained supervision improves policy learning in simulation (RoboTwin, Section 4.3), and (3) whether the resulting policies exhibit steerable control on real-world dual-arm manipulation (Section 4.4).

4.1 Experimental Setup

Evaluation benchmark. We evaluate FineVLA on three complementary evaluation protocols that measure robotic video understanding, simulated policy learning, and physical steerable control.

(1) RoboFine-Bench. RoboFine-Bench (Section 2.3) evaluates whether RoboFine-VLM captures fine-grained robotic action details. We compare RoboFine-VLM with five strong general-purpose VLMs on both VQA and captioning tracks. The VQA track reports overall and dimension-wise accuracy across the ten FineVLA dimensions, while the captioning track scores ordered step-level action descriptions using Consistency, Coverage, and Anti-Hallucination metrics.

(2) RoboTwin Simulation Evaluation. RoboTwin (21) evaluates simulated bimanual manipulation. We test the seven FG:Raw instruction ratios defined in Section 3.2 across three controlled policy settings: RDT-OFT, RDT-GR00T, and AlohaMix-OFT. Policies are evaluated on the official Easy and Hard splits, with 20 episodes per task.

(3) Real-world Steerability Evaluation. We design this self-contained real-world benchmark on a Cobot Magic dual-arm platform to measure language-conditioned controllability. Unlike broad robustness benchmarks that vary scenes, objects, or lighting, our suite isolates instruction following: for each instruction-sensitive task family, paired variants use the same object set and nearly identical initial scene layout while changing only one language-specified control factor. The suite includes two general manipulation tasks, five in-distribution instruction-sensitive task families (each comprising a paired variant) covering object color, object pose, approach direction, rotation direction, and active arm, and one out-of-distribution active-arm–target binding probe. Each paired variant is evaluated over 10 trials and scored with a partial-completion rubric normalized to a 0–100 scale. Additional hardware and inference details are reported in Appendix A.6.1.

Training setup. We train three policy configurations—**RDT-OFT**, **RDT-GR00T**, and **AlohaMix-OFT**—to decouple architecture and data-mixture effects. RDT-OFT and RDT-GR00T use the same RDT pretraining data with different action decoders, while RDT-OFT and AlohaMix-OFT use the same OFT decoder with different pretraining mixtures. We pretrain each configuration for 100k steps on 64 A100 GPUs with per-device batch size 8 and global batch size 512.

For RoboTwin evaluation, we fine-tune the pretrained checkpoints on the union of the Clean and Random training sets, containing 27,500 trajectories and 6,075,103 transitions, for 100k steps on

Table 2: **VQA benchmark results on RoboFine-Bench (%)**. We report overall VQA accuracy together with all ten fine-grained capability dimensions. **AA**: Active Actor; **TO**: Target Object; **IC**: Initial Configuration; **AS**: Action Sequence; **C&A**: Contact & Approach; **T&O**: Trajectory & Orientation; **BM**: Body Motion; **OI**: Object Interaction; **FC**: Final Configuration; **F&R**: Failure & Recovery. Best value per column is **bold**.

Model	Overall↑	Gnd.↑			Act.↑				State↑		
		AA	TO	IC	AS	C&A	T&O	BM	OI	FC	F&R
Qwen3-VL-Plus	50.4	68.9	51.8	55.0	62.1	43.0	43.7	63.6	50.0	46.0	50.0
Qwen3.5-Plus	52.6	70.5	47.1	62.5	55.0	45.5	47.4	72.7	26.9	58.4	42.9
Doubao-Seed-2.0-Pro	54.9	60.7	55.3	61.3	61.4	50.0	45.1	72.7	42.3	61.6	50.0
Gemini-3.1-Pro	62.1	83.6	67.1	68.8	72.9	52.6	52.1	63.6	23.1	67.6	50.0
GPT-5.4	61.0	85.1	60.0	58.8	66.4	61.5	50.7	63.6	50.0	65.4	28.6
RoboFine-VLM (Ours)	71.0	85.2	63.5	72.5	73.6	67.3	56.7	81.8	57.7	66.5	85.7

Table 3: **Caption benchmark results on RoboFine-Bench (%)**. We report caption quality under two settings: **easy**, where the original task instruction is provided, and **hard**, where the model must infer the manipulation process from vision alone. **Cons.:** Consistency; **Cov.:** Coverage; **A-Hal.:** Anti-Hallucination. Best value per column is **bold**.

Model	Easy				Hard			
	Overall↑	Cons.↑	Cov.↑	A-Hal.↑	Overall↑	Cons.↑	Cov.↑	A-Hal.↑
Qwen3-VL-Plus	76.8	75.6	60.4	94.4	65.1	68.7	57.0	69.6
Qwen3.5-Plus	77.9	76.0	61.7	96.0	72.5	70.9	56.8	89.7
Doubao-Seed-2.0-Pro	80.2	79.6	72.1	88.9	68.2	72.2	65.6	66.8
Gemini-3.1-Pro	81.3	80.8	69.8	93.2	77.2	77.0	61.3	93.4
GPT-5.4	83.1	80.8	75.1	93.4	78.1	74.2	68.9	91.1
RoboFine-VLM (Ours)	85.2	83.9	76.7	95.1	83.6	81.9	75.3	93.7

8 A100 GPUs with global batch size 128. The FG:Raw instruction mixture is applied during this fine-tuning stage; pretraining uses the original instruction format of each source dataset.

For real-world evaluation, we further fine-tune the corresponding simulation checkpoint for each instruction-mixture setting on 50 demonstrations per task from 12 tabletop tasks, for 600 demonstrations in total, collected on the Cobot Magic dual-arm platform. Full optimizer, hardware, batch-size, and training-step configurations are reported in Appendix A.4, Table 20.

4.2 RoboFine-Bench Results

Tables 2 and 3 compare RoboFine-VLM with five strong general-purpose VLMs on RoboFine-Bench. A more detailed analysis of the benchmark results is provided in Appendix A.3.8.

VQA results. RoboFine-VLM achieves **71.0%** overall accuracy, outperforming the strongest general-purpose baseline, Gemini-3.1-Pro, by **8.9** absolute points. The largest gain appears on Action and Motion Understanding (**68.4%** vs. **58.4%**), indicating that fine-grained supervision improves execution-level reasoning beyond scene recognition. Compared with its base model Qwen3.5-Plus (i.e., Qwen3.5-397B-A17B), SFT on FineVLA-Data improves overall accuracy from **52.6%** to **71.0%**, with consistent gains across grounding, action, and state reasoning.

Caption results. RoboFine-VLM also leads the caption track. In the easy setting, where the task instruction is provided, it obtains the best Overall, Consistency, and Coverage scores. In the hard setting, where the model must infer the manipulation process from video alone, RoboFine-VLM ranks first on all four metrics and improves Overall from the strongest baseline score of **78.1%** to **83.6%**. This setting is especially important because it measures whether the model captures the execution process rather than relying on task-level language priors. Token and latency statistics are reported in Appendix A.3.7.

Benchmark validity. The caption ranking is robust to the choice of alignment judge: replacing GPT-5.4-Pro with Gemini-3.1-Pro yields the same model ranking in both easy and hard settings, with only small changes in absolute scores (Appendix A.3.5). The automatic scores also align strongly

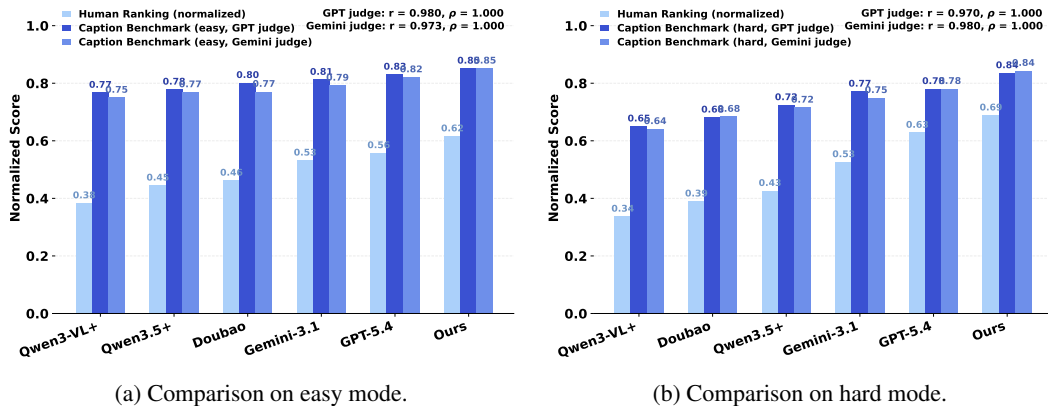


Figure 4: **Correlation between benchmark caption scores and human ranking.** We recruit 10 human raters to rank the six models on the 500 benchmark videos, and average the resulting subjective scores. Human ranks are normalized from the 1–6 range to $[0, 1]$, while benchmark caption Overall scores are normalized from 0–100 to $[0, 1]$.

Table 4: **RoboTwin simulation success rate (%)**. We compare three training settings (RDT-OFT, RDT-GR00T, and AlohaMix-OFT) under seven FG:Raw instruction ratios. Easy/Hard follow the official RoboTwin splits. Best value per column is **bold**.

FG:Raw	RDT-OFT		RDT-GR00T		AlohaMix-OFT	
	Easy \uparrow	Hard \uparrow	Easy \uparrow	Hard \uparrow	Easy \uparrow	Hard \uparrow
Raw-only	61.5	60.0	55.1	53.4	71.8	71.4
FG : Raw = 1 : 4	68.2	66.5	58.2	55.7	75.3	74.3
FG : Raw = 1 : 2	74.1	72.1	61.7	60.9	82.8	78.6
FG : Raw = 1 : 1	73.9	72.4	69.4	68.2	86.8	82.5
FG : Raw = 2 : 1	70.4	68.3	65.9	63.1	80.9	79.3
FG : Raw = 4 : 1	68.6	67.5	64.9	63.2	79.5	78.5
FG-only	62.9	62.0	62.1	61.5	78.3	76.1

with human preference. As shown in Figure 4, the correlation between benchmark Overall scores and the rankings from 10 human raters is high in both settings (easy: Pearson **0.980**, Spearman ρ **1.000**; hard: Pearson **0.970**, Spearman ρ **1.000**).

These results provide evidence that RoboFine-VLM can produce dense, action-aligned robotic descriptions, and that the proposed annotation schema captures execution-level manipulation details. Importantly, the fine-grained supervision used for policy training is produced by FineVLA-Tool with human verification, rather than by RoboFine-VLM. Thus, RoboFine-VLM is evaluated here as a scalable annotator for future data expansion.

4.3 RoboTwin Simulation Results

We evaluate on RoboTwin (21), a simulation benchmark for bimanual manipulation, and report success rate on its official **Easy** and **Hard** splits. Each policy is evaluated over 20 episodes per task and averaged to produce the per-split score. Table 4 reports results across three (dataset, framework) combinations: RDT-OFT, RDT-GR00T, and AlohaMix-OFT. Note that AlohaMix is approximately $13\times$ larger than RDT in episode count, enabling a controlled study of data-scale effects.

Table 4 shows two main results. First, fine-grained supervision does not harm goal-level task success: FG-only improves over Raw-only across all evaluated settings, with gains of $+1.4/+2.0$ on RDT-OFT (Easy/Hard), $+7.0/+8.1$ on RDT-GR00T, and $+6.5/+4.7$ on AlohaMix-OFT. Second, fine-grained and raw instructions are complementary: as the FG proportion increases from 0% to 100%, success rate follows a consistent inverted-U trend across all three settings, peaking around FG : Raw = 1 : 2 to 1 : 1. The best setting, FG : Raw = 1 : 1, reaches **86.8%/82.5%** on AlohaMix-OFT Easy/Hard, a gain of $+15.0/+11.1$ over the Raw-only baseline (71.8%/71.4%). Both conclusions hold across all three

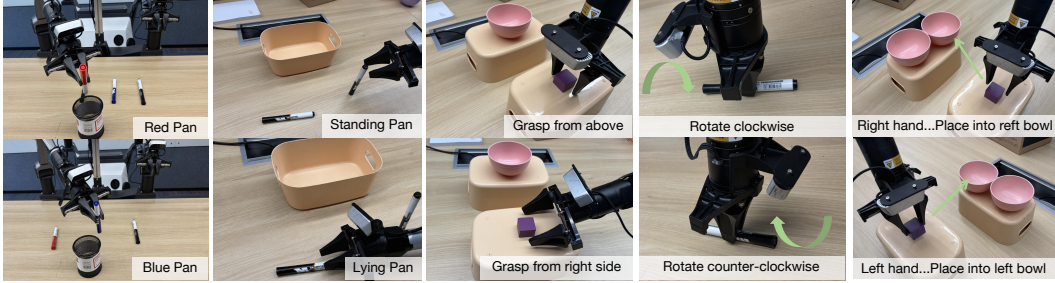


Figure 5: **Paired real-world evaluation.** Each column shows one control factor under the same visual scene with two language variants. From left to right: Color (red/blue), Pose (standing/lying), Approach (above/side), Rotation (clockwise/counterclockwise), Arm (right/left).

Table 5: **Real-world scores on a 100-point scale.** All models use StarVLA-OFT pretrained on AlohaMix (100k fine-tuning steps). Each trial is scored by manually checking ordered subgoals; a completed subgoal receives proportional credit, and the final score is normalized to 100. *Avg (ID)* averages the seven in-distribution tasks; *Avg (All)* includes the OOD probe (\dagger). **Bold** indicates the best score per column. Task descriptions and control factors are listed in Table 24.

Supervision	In-Distribution Tasks							OOD	Average	
	Clean Table	Stack Block	Color	Pose	Approach	Rotate	Arm		$L \rightarrow R^\dagger$ (ID)	(All)
Raw-only	72	35	22	24	60	76	60	0	49.9	43.6
FG : Raw = 1 : 4	76	36	28	32	65	79	61	0	53.9	47.1
FG : Raw = 1 : 2	79	39	36	48	76	87	63	5	61.1	54.1
FG : Raw = 1 : 1	84	40	40	47	78	86	64	10	62.7	56.1
FG : Raw = 2 : 1	80	38	34	42	72	83	62	5	58.7	52.0
FG : Raw = 4 : 1	74	37	31	43	72	83	62	5	57.4	50.9
FG-only	70	35	25	41	70	80	60	0	54.4	47.6

$\dagger L \rightarrow R$: use left hand to place into right bowl; unseen actor-target combination (OOD compositional probe). Control factors are detailed in Appendix A.6.1.

(dataset, framework) combinations, regardless of action-decoding architecture (OFT vs. GR00T) and pretraining data scale (RDT vs. AlohaMix). We analyze this trend and its mechanism in Section 5.2.

4.4 Real-World Steerability Results

We evaluate physical steerable control on our self-designed Real-world Steerability Suite (Figure 5). This benchmark is designed to isolate language-conditioned controllability: paired task variants share nearly the same visual scene but require different behaviors according to the instruction, such as choosing a different object color, object pose, approach direction, rotation direction, or active arm.

Table 5 shows two main results. First, fine-grained supervision improves steerable control—a conclusion that simulation benchmarks alone cannot provide. $FG : Raw = 1 : 1$ improves every instruction-sensitive factor over Raw-only: Color (22 \rightarrow **40**), Pose (24 \rightarrow **47**), Approach (60 \rightarrow **78**), Rotate (76 \rightarrow **86**), and Arm (60 \rightarrow **64**). The largest gains appear on factors invisible to goal-level language—Pose (+23), Color and Approach (+18 each)—precisely the execution choices that raw instructions leave unspecified. Second, consistent with the simulation findings, fine-grained and raw instructions are complementary in the real world. The in-domain score follows a clear inverted-U trend across all seven settings (49.9 \rightarrow 53.9 \rightarrow 61.1 \rightarrow **62.7** \rightarrow 58.7 \rightarrow 57.4 \rightarrow 54.4), peaking at $FG : Raw = 1 : 1$ (**62.7/100**), which outperforms both Raw-only (49.9) and FG-only (54.4). On the two general manipulation tasks, Clean Table (72 \rightarrow **84**) and Stack Block (35 \rightarrow **40**), mixed supervision also matches or exceeds Raw-only, indicating that process-level language does not interfere with routine execution. The OOD actor-target binding remains challenging, but the mixed model improves from 0 to 10/100, suggesting partial factor-level generalization. We analyze factor-level controllability and failure modes in Section 5.4.

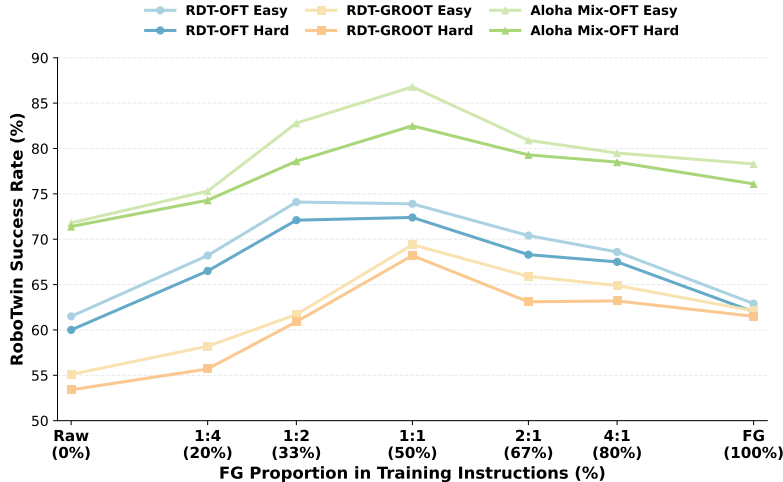


Figure 6: **RoboTwin mixing-ratio curves.** Performance peaks around FG : Raw = 1 : 2 to 1 : 1 across all settings, yielding a consistent inverted-U trend.

5 Analysis

This section analyzes *why* fine-grained supervision improves performance, how it should be mixed with raw goal-level instructions, and which control factors benefit most from action-aligned language.

5.1 Fine-Grained Supervision Does Not Sacrifice Goal-Level Success

A natural concern is that fine-grained instructions may over-specify execution details and distract the policy from completing the high-level goal. Our results suggest the opposite. In RoboTwin (Table 4), FG-only improves over Raw-only across all three (dataset, framework) combinations, with gains ranging from +1.4/+2.0 (RDT-OFT, Easy/Hard) to +7.0/+8.1 (RDT-GROOT) and +6.5/+4.7 (AlohaMix-OFT). In the real-world evaluation (Table 5), mixed supervision also matches or exceeds Raw-only on the two general manipulation tasks (Clean Table, Stack Block), where no fine-grained control factor is explicitly tested. The pattern holds regardless of decoder architecture (OFT vs. GROOT), pretraining data scale (RDT vs. AlohaMix), and environment (simulation vs. physical), indicating that process-level language provides additional action constraints without sacrificing goal-level task completion.

5.2 Raw and Fine-Grained Supervision Are Complementary

Although FG-only outperforms Raw-only, the *best* performance is achieved by mixing both supervision types. As the FG proportion increases from 0% to 100%, success rate traces a clear inverted-U curve in all three RoboTwin settings, peaking around FG : Raw = 1 : 2 to 1 : 1 (Figure 6). The same trend transfers to the real world (Table 5): FG : Raw = 1 : 1 achieves the highest in-domain score (62.7/100), outperforming both Raw-only (49.9) and FG-only (54.4).

We attribute this inverted-U to the complementary roles of the two instruction types. Raw instructions preserve compact goal semantics—*what* task should be completed—while fine-grained instructions expose execution constraints—*how* the task should be performed. Under *Raw-only*, execution-level choices (arm, approach, rotation) are left to implicit co-occurrence statistics. Under *FG-only*, the policy has explicit process-level guidance, but losing goal-level abstractions may weaken generalization to instruction phrasings not seen during training. In addition, FG descriptions are longer and more distributionally different from natural user commands, so training exclusively on FG language may reduce exposure to compact goal-level task phrasing. Under *Mixed* supervision, the policy simultaneously learns task semantics from raw instructions and execution constraints from fine-grained descriptions, retaining the strengths of both. The inverted-U trend suggests that fine-grained language should augment, not replace, raw task instructions.

5.3 Architecture and Data-Scale Effects

FG supervision narrows the architecture gap. Comparing StarVLA-OFT and StarVLA-GR00T on the same dataset (RDT), OFT is clearly stronger under Raw-only supervision (gap of 6.4/6.6 on Easy/Hard), but the gap shrinks as FG ratio increases and nearly vanishes under FG-only (0.8/0.5). This suggests that dense language supervision alleviates a supervision bottleneck, reducing the policy’s dependence on decoder architecture choice.

FG supervision benefits more from larger data scale. Comparing RDT-OFT and AlohaMix-OFT, the gain from FG supervision is larger on the bigger AlohaMix dataset. The FG-only improvement over Raw-only grows from +1.4/+2.0 (RDT) to +6.5/+4.7 (AlohaMix). As trajectory diversity grows, dense action-aligned language has more distinct execution patterns to bind to. Together with the architecture result above, this suggests that fine-grained supervision is not merely an incidental improvement for current-scale training: it represents a scalable supervision axis beyond a single architecture or dataset scale.

Detailed per-setting numbers supporting both observations are reported in Appendix A.5, Table 23.

5.4 Fine-Grained Language Enables Factor-Level Steerable Control

Overall task success can hide instruction violations: a policy may complete the goal-level task while using the wrong arm, approaching from the wrong direction, or rotating in the wrong direction. We therefore examine the five single-factor columns in Table 5, where each column isolates exactly one language-specified control attribute while holding the visual scene fixed.

Table 5 shows that FG : Raw = 1 : 1 improves every instruction-sensitive factor over Raw-only. The largest gains appear on attributes invisible to goal-level language: Pose (24 → 47, +23), Color (22 → 40, +18), and Approach (60 → 78, +18). Rotate improves from 76 to 86 (+10), and Arm from 60 to 64 (+4). The gain magnitude correlates with how much each factor is underspecified by raw instructions: object pose, color, and approach direction receive no guidance in goal-level language, while rotation direction and arm selection are occasionally implied by task context. These results show that fine-grained supervision improves not only overall task completion, but also execution compliance on the specific control attribute specified by the instruction.

The OOD actor-target probe reveals a different pattern. The FG : Raw = 1 : 2 and 1 : 1 settings achieve the highest OOD scores (5 and 10 respectively), compared with 0 for Raw-only, suggesting that mixed supervision strengthens individual factor grounding. However, this does not translate into full task completion because the policy still fails to bind the selected arm to the unseen target receptacle. Thus, FineVLA improves factor-level controllability, but full compositional generalization remains unsolved.

5.5 Limitations

The remaining real-world failures fall into two categories. The first is *grounding failure*, where the policy selects the wrong object, arm, or target despite the language specifying the correct factor. The second is *execution failure*, where the correct factor is selected but the physical manipulation fails, such as unstable grasping, incomplete rotation, or inaccurate placement. The OOD actor-target probe further shows a compositional limitation: increasing FG supervision improves active-arm grounding, but does not reliably solve novel actor-target binding.

Our framework also has several limitations. RoboFine-VLM reduces annotation cost but does not fully remove human verification. Real-world validation is still limited to a tabletop dual-arm platform and a small set of targeted steerability tasks. Finally, following fine-grained execution instructions in physical environments raises safety concerns; future systems should combine fine-grained language following with feasibility and safety checks.

6 Related Work

VLA policy learning and sparse trajectory language. Recent VLA policies such as RT-2 (22), OpenVLA (23), π_0 (24), and Octo (25) leverage pretrained vision-language models and large demonstration datasets such as Open X-Embodiment (5), DROID (19), and BridgeData V2 (11). While these

efforts substantially improve generalist policy learning, their paired language supervision remains sparse: each trajectory is annotated with a goal-level task name that specifies the desired outcome but omits execution details such as which arm to use, how to approach the object, or what motion path to follow.

Fine-grained supervision for manipulation. Several works enrich supervision beyond trajectory-level labels. Galaxea (14), RoboCOIN (17), and RoboInter (26) introduce subtask or hierarchical annotations; STEER (27) and PartInstruct (28) study low-level or part-level instruction following. These annotations are typically organized around stages, primitives, or object parts rather than full process-level descriptions. FineVLA instead provides process-level, action-aligned supervision across a ten-dimensional schema that unifies actor choice, contact patterns, motion trajectories, state transitions, and recovery behavior—and uses this supervision consistently for data construction, VLM training, benchmark evaluation, and policy learning.

Robotic video understanding and scalable annotation. General video-language models such as Qwen3-VL (29) and Qwen3.5-Omni (30) provide strong foundations for video captioning, while embodied benchmarks such as RoboVQA (7), RoboBench (8), and HanDyVQA (9) evaluate spatial reasoning, affordances, and hand-object dynamics. Dense captioning methods such as Wolf (31), DIAL (32), and RoboAnnotatorX (33) further improve annotation scalability. However, general captions do not necessarily align with robot action. FineVLA closes this gap by connecting robotic video understanding directly to VLA policy learning: RoboFine-VLM generates action-aligned descriptions, RoboFine-Bench evaluates execution-level understanding, and FineVLA-Policy tests whether such supervision improves instruction-sensitive control.

Steerable robot foundation models. Recent robot foundation models increasingly emphasize instruction-steerable behavior, where policies should follow not only task goals but also execution-level constraints (1, 2, 3, 4). However, the data construction and evaluation infrastructure behind many such systems remains limited or closed. FineVLA complements these efforts by providing an open action-aligned annotation pipeline, a held-out benchmark, a scalable annotator, and a controlled policy-training study.

7 Conclusion

We presented **FineVLA**, a framework that reframes steerable VLA learning as an action-instruction alignment problem: language supervision should specify not only *what* task to complete, but also the execution-level choices that determine *how* the robot completes it.

Starting from 972,247 trajectories across 10 open-source datasets, FineVLA-Tool produces 47,159 human-verified trajectories with process-level annotations spanning ten fine-grained dimensions. RoboFine-VLM, fine-tuned on this data, serves as a scalable annotator that achieves 71.0% VQA accuracy and 83.6% captioning score on the held-out RoboFine-Bench. FineVLA-Policy, trained under controlled FG:Raw instruction mixtures, reaches **86.8%/82.5%** on AlohaMix-OFT Easy/Hard in RoboTwin simulation, and **62.7/100** in real-world dual-arm manipulation (vs. 49.9 for Raw-only), with the largest per-factor gains on execution-sensitive attributes such as pose (+23), color (+18), and approach direction (+18).

Two key findings emerge. First, fine-grained supervision does not sacrifice goal-level task success; it consistently improves over raw-only baselines across architectures, data scales, and environments. Second, fine-grained and raw instructions are complementary: the inverted-U trend across all settings shows that the best steerable control comes from mixing both—raw instructions specify *what* to achieve, while fine-grained descriptions specify *how* to execute it. Third, fine-grained supervision directly improves factor-level steerable control: in real-world evaluation, the largest gains appear on execution-sensitive attributes such as color, pose, and approach direction, where goal-level instructions provide no guidance.

We release FineVLA-Tool, RoboFine-VLM, RoboFine-Bench, and FineVLA-Policy checkpoints and training code to support reproducible research on steerable VLA policies. Remaining challenges include compositional generalization to unseen instruction combinations, validation across broader embodiments and task domains, and integrating feasibility and safety checks for fine-grained language following in physical deployment.

References

- [1] Physical Intelligence, Bo Ai, Ali Amin, Raichelle Aniceto, Ashwin Balakrishna, Greg Balke, Kevin Black, George Bokinsky, Shihao Cao, Thomas Charbonnier, Vedant Choudhary, Foster Collins, Ken Conley, Grace Connors, James Darpinian, Karan Dhabalia, Maitrayee Dhaka, Jared DiCarlo, Danny Driess, Michael Equi, Adnan Esmail, Yunhao Fang, Chelsea Finn, Catherine Glossop, Thomas Godden, Ivan Goryachev, Lachlan Groom, Haroun Habeeb, Hunter Hancock, Karol Hausman, Gashon Hussein, Victor Hwang, Brian Ichter, Connor Jacobsen, Szymon Jakubczak, Rowan Jen, Tim Jones, Gregg Kammerer, Ben Katz, Liyiming Ke, Mairbek Khadikov, Chandra Kuchi, Marinda Lamb, Devin LeBlanc, Brendon LeCount, Sergey Levine, Xinyu Li, Adrian Li-Bell, Vladislav Lialin, Zhonglin Liang, Wallace Lim, Yao Lu, Enyu Luo, Vishnu Mano, Nandan Marwaha, Aikys Mongush, Liam Murphy, Suraj Nair, Tyler Patterson, Karl Pertsch, Allen Z. Ren, Gavin Schelske, Charvi Sharma, Baifeng Shi, Lucy Xiaoyang Shi, Laura Smith, Jost Tobias Springenberg, Kyle Stachowicz, Will Stoeckle, Jiaming Tang, Jimmy Tanner, Shalom Tekeste, Marcel Torne, Kyle Vedder, Quan Vuong, Anna Walling, Haohuan Wang, Jason Wang, XuDong Wang, Chris Whalen, Samuel Whitmore, Blake Williams, Charles Xu, Sukwon Yoo, Lili Yu, Wuming Zhang, Zhuoyang Zhang, and Ury Zhilinsky. $\pi_{0.7}$: a steerable generalist robotic foundation model with emergent capabilities, 2026. URL <https://arxiv.org/abs/2604.15483>.
- [2] Wei Wu, Fan Lu, Yunnan Wang, Shuai Yang, Shi Liu, Fangjing Wang, Qian Zhu, He Sun, Yong Wang, Shuailei Ma, Yiyu Ren, Kejia Zhang, Hui Yu, Jingmei Zhao, Shuai Zhou, Zhenqi Qiu, Houlong Xiong, Ziyu Wang, Zechen Wang, Ran Cheng, Yong-Lu Li, Yongtao Huang, Xing Zhu, Yujun Shen, and Kecheng Zheng. A pragmatic v1a foundation model, 2026. URL <https://arxiv.org/abs/2601.18692>.
- [3] NVIDIA. Nvidia isaac gr00t. <https://github.com/NVIDIA/Isaac-GR00T>, 2026. GitHub repository, accessed April 13, 2026.
- [4] Generalist AI. Gen-1. <https://generalistai.com/blog/apr-02-2026-GEN-1>, 2026. Blog post, accessed April 2, 2026.
- [5] Open X-Embodiment Collaboration. Open X-Embodiment: Robotic learning datasets and RT-X models, 2023. URL <https://arxiv.org/abs/2310.08864>.
- [6] Songming Liu, Lingxuan Wu, Bangguo Li, Hengkai Tan, Huayu Chen, Zhengyi Wang, Ke Xu, Hang Su, and Jun Zhu. Rdt-1b: a diffusion foundation model for bimanual manipulation, 2025. URL <https://arxiv.org/abs/2410.07864>.
- [7] Pierre Sermanet, Tianli Ding, Jeffrey Zhao, Fei Xia, Debidatta Dwibedi, Keerthana Gopalakrishnan, Christine Chan, Gabriel Dulac-Arnold, Sharath Maddineni, Nikhil J. Joshi, Pete Florence, Wei Han, Robert Baruch, Yao Lu, Suvir Mirchandani, Peng Xu, Pannag Sanketi, Karol Hausman, Izhak Shafran, Brian Ichter, and Yuan Cao. RoboVQA: Multimodal long-horizon reasoning for robotics, 2023. URL <https://arxiv.org/abs/2311.00899>.
- [8] Yulin Luo, Chun-Kai Fan, Menghang Dong, Jiayu Shi, Mengdi Zhao, Bo-Wen Zhang, Cheng Chi, Jiaming Liu, Gaole Dai, Rongyu Zhang, Ruichuan An, Kun Wu, Zhengping Che, Shaoxuan Xie, Guocai Yao, Zhongxia Zhao, Pengwei Wang, Guang Liu, Zhongyuan Wang, Tiejun Huang, and Shanghang Zhang. Robobench: A comprehensive evaluation benchmark for multimodal large language models as embodied brain, 2025. URL <https://arxiv.org/abs/2510.17801>.
- [9] Masatoshi Tateno, Gido Kato, Hirokatsu Kataoka, Yoichi Sato, and Takuma Yagi. HanDyVQA: A video QA benchmark for fine-grained hand-object interaction dynamics, 2025. URL <https://arxiv.org/abs/2512.00885>.
- [10] Qwen Team. Qwen3.5: Towards native multimodal agents, February 2026. URL <https://qwen.ai/blog?id=qwen3.5>.
- [11] Homer Walke, Kevin Black, Abraham Lee, Moo Jin Kim, Max Du, Chongyi Zheng, Tony Zhao, Philippe Hansen-Estruch, Quan Vuong, Andre He, et al. BridgeData V2: A dataset for robot learning at scale. In *Proceedings of the Conference on Robot Learning*, 2023. URL <https://arxiv.org/abs/2308.12952>.

- [12] Eric Jang, Alex Irpan, Mohi Khansari, Daniel Kappler, Frederik Ebert, Corey Lynch, Sergey Levine, and Chelsea Finn. Bc-z: Zero-shot task generalization with robotic imitation learning, 2022. URL <https://arxiv.org/abs/2202.02005>.
- [13] Anthony Brohan, Yevgen Chebotar, Chelsea Finn, Karol Hausman, Alexander Herzog, Daniel Ho, Julian Ibarz, Alex Irpan, Eric Jang, Ryan Julian, et al. RT-1: Robotics transformer for real-world control at scale, 2022. URL <https://arxiv.org/abs/2212.06817>.
- [14] Tao Jiang, Tianyuan Yuan, Yicheng Liu, Chenhao Lu, et al. Galaxea open-world dataset and G0 dual-system VLA model, 2025. URL <https://arxiv.org/abs/2509.00576>.
- [15] Kun Wu, Chengkai Hou, Jiaming Liu, Zhengping Che, Xiaozhu Ju, Zhuqin Yang, Meng Li, YINUO Zhao, Zhiyuan Xu, Guang Yang, Shichao Fan, Xinhua Wang, Fei Liao, Zhen Zhao, Guangyu Li, Zhao Jin, Lecheng Wang, Jilei Mao, Ning Liu, Pei Ren, Qiang Zhang, Yaoxu Lyu, Mengzhen Liu, He Jingyang, Yulin Luo, Zeyu Gao, Chenxuan Li, Chenyang Gu, Yankai Fu, Di Wu, Xingyu Wang, Sixiang Chen, Zhenyu Wang, Pengju An, Siyuan Qian, Shanghang Zhang, and Jian Tang. RoboMIND: Benchmark on multi-embodiment intelligence normative data for robot manipulation. In *Robotics: Science and Systems XXI*, RSS2025. Robotics: Science and Systems Foundation, June 2025. doi: 10.15607/rss.2025.xxi.152. URL <http://dx.doi.org/10.15607/RSS.2025.XXI.152>.
- [16] Chengkai Hou, Kun Wu, Jiaming Liu, Zhengping Che, et al. RoboMIND 2.0: A multimodal, bimanual mobile manipulation dataset for generalizable embodied intelligence, 2025. URL <https://arxiv.org/abs/2512.24653>.
- [17] Shihan Wu, Xuecheng Liu, Shaoxuan Xie, Pengwei Wang, et al. RoboCOIN: An open-sourced bimanual robotic data collection for integrated manipulation, 2025. URL <https://arxiv.org/abs/2511.17441>.
- [18] Hao-Shu Fang, Hongjie Fang, Zhenyu Tang, Jirong Liu, Chenxi Wang, Junbo Wang, Haoyi Zhu, and Cewu Lu. Rh20t: A comprehensive robotic dataset for learning diverse skills in one-shot, 2023. URL <https://arxiv.org/abs/2307.00595>.
- [19] Alexander Khazatsky, Karl Pertsch, Suraj Nair, Ashwin Balakrishna, Sudeep Dasari, Siddharth Karamcheti, Soroush Nasiriany, Mohan Kumar Srirama, Lawrence Yunliang Chen, Kirsty Ellis, et al. DROID: A large-scale in-the-wild robot manipulation dataset, 2024. URL <https://arxiv.org/abs/2403.12945>.
- [20] StarVLA Community. Starvla: A lego-like codebase for vision-language-action model developing, 2026. URL <https://arxiv.org/abs/2604.05014>.
- [21] Yao Mu, Tianxing Chen, Shijia Peng, Zanxin Chen, Zeyu Gao, Yude Zou, Lunkai Lin, Zhiqiang Xie, and Ping Luo. RoboTwin: Dual-arm robot benchmark with generative digital twins, 2024. URL <https://arxiv.org/abs/2409.02920>.
- [22] Anthony Brohan, Noah Brown, Justice Carbajal, Yevgen Chebotar, Xi Chen, Krzysztof Choromanski, Tianli Ding, Danny Driess, Avinava Dubey, Chelsea Finn, et al. RT-2: Vision-language-action models transfer web knowledge to robotic control, 2023. URL <https://arxiv.org/abs/2307.15818>.
- [23] Moo Jin Kim, Karl Pertsch, Siddharth Karamcheti, Ted Xiao, Ashwin Balakrishna, Suraj Nair, Rafael Rafailov, Ethan Foster, Grace Lam, Pannag Sanketi, et al. OpenVLA: An open-source vision-language-action model, 2024. URL <https://arxiv.org/abs/2406.09246>.
- [24] Kevin Black, Noah Brown, Danny Driess, Adnan Esmail, Michael Equi, Chelsea Finn, Niccolo Fusai, Lachy Groom, Karol Hausman, Brian Ichter, et al. π_0 : A vision-language-action flow model for general robot control, 2024. URL <https://arxiv.org/abs/2410.24164>.
- [25] Octo Model Team, Dibya Ghosh, Homer Walke, Karl Pertsch, Kevin Black, Oier Mees, Sudeep Dasari, Joey Hejna, Tobias Kreiman, Charles Xu, Jianlan Luo, You Liang Tan, Lawrence Yunliang Chen, Pannag Sanketi, Quan Vuong, Ted Xiao, Dorsa Sadigh, Chelsea Finn, and Sergey Levine. Octo: An open-source generalist robot policy, 2024. URL <https://arxiv.org/abs/2405.12213>.

- [26] Hao Li, Ziqin Wang, Zi-han Ding, Shuai Yang, et al. RoboInter: A holistic intermediate representation suite towards robotic manipulation, 2026. URL <https://arxiv.org/abs/2602.09973>.
- [27] Laura Smith, Alex Irpan, Montserrat Gonzalez Arenas, Sean Kirmani, Dmitry Kalashnikov, Dhruv Shah, and Ted Xiao. STEER: Flexible robotic manipulation via dense language grounding, 2024. URL <https://arxiv.org/abs/2411.03409>.
- [28] Yifan Yin, Zhengtao Han, Shivam Aarya, Jianxin Wang, Shuhang Xu, Jiawei Peng, Angtian Wang, Alan Yuille, and Tianmin Shu. PartInstruct: Part-level instruction following for fine-grained robot manipulation, 2025. URL <https://arxiv.org/abs/2505.21652>.
- [29] Shuai Bai, Yuxuan Cai, Ruizhe Chen, Keqin Chen, Xionghui Chen, Zesen Cheng, Lianghao Deng, Wei Ding, Chang Gao, Chunjiang Ge, Wenbin Ge, Zhifang Guo, Qidong Huang, Jie Huang, Fei Huang, Binyuan Hui, Shutong Jiang, Zhaohai Li, Mingsheng Li, Mei Li, Kaixin Li, Zicheng Lin, Junyang Lin, Xuejing Liu, Jiawei Liu, Chenglong Liu, Yang Liu, Dayiheng Liu, Shixuan Liu, Dunjie Lu, Ruilin Luo, Chenxu Lv, Rui Men, Lingchen Meng, Xuancheng Ren, Xingzhang Ren, Sibao Song, Yuchong Sun, Jun Tang, Jianhong Tu, Jianqiang Wan, Peng Wang, Pengfei Wang, Qiuyue Wang, Yuxuan Wang, Tianbao Xie, Yiheng Xu, Haiyang Xu, Jin Xu, Zhibo Yang, Mingkun Yang, Jianxin Yang, An Yang, Bowen Yu, Fei Zhang, Hang Zhang, Xi Zhang, Bo Zheng, Humen Zhong, Jingren Zhou, Fan Zhou, Jing Zhou, Yuezhi Zhu, and Ke Zhu. Qwen3-VL technical report, 2025. URL <https://arxiv.org/abs/2511.21631>.
- [30] Qwen Team. Qwen3.5-Omni technical report, 2026. URL <https://arxiv.org/abs/2604.15804>.
- [31] Boyi Li, Ligeng Zhu, Ran Tian, Shuhan Tan, Yuxiao Chen, Yao Lu, Yin Cui, Sushant Veer, Max Ehrlich, Jonah Philion, Xinshuo Weng, Fuzhao Xue, Linxi Fan, Yuke Zhu, Jan Kautz, Andrew Tao, Ming-Yu Liu, Sanja Fidler, Boris Ivanovic, Trevor Darrell, Jitendra Malik, Song Han, and Marco Pavone. Wolf: Dense video captioning with a world summarization framework, 2025. URL <https://arxiv.org/abs/2407.18908>.
- [32] Ted Xiao, Harris Chan, Pierre Sermanet, Ayzaan Wahid, Anthony Brohan, Karol Hausman, Sergey Levine, and Jonathan Tompson. Robotic skill acquisition via instruction augmentation with vision-language models. In *Robotics: Science and Systems*, 2023. URL <https://arxiv.org/abs/2211.11736>.
- [33] Longxin Kou, Fei Ni, Yan Zheng, Peilong Han, Jinyi Liu, Haiqin Cui, Rui Liu, and Jianye Hao. RoboAnnotatorX: A comprehensive and universal annotation framework for accurate understanding of long-horizon robot demonstration. In *Proceedings of the IEEE/CVF International Conference on Computer Vision*, pages 10353–10363, 2025. URL https://openaccess.thecvf.com/content/ICCV2025/html/Kou_RoboAnnotatorX_A_Comprehensive_and_Universal_Annotation_Framework_for_Accurate_Understanding_ICCV_2025_paper.html.

A Appendix

Contents

A.1	FineVLA-Tool Details	18
A.1.1	Data Sources and Format Conversion	18
A.1.2	Action-State Canonicalization	18
A.1.3	Quality Filtering and DTW Consistency Check	19
A.1.4	Action-Based Clustering and Representative Sampling	19
A.1.5	Fine-Grained Annotation Schema	21
A.1.6	Human-in-the-Loop Verification	23
A.2	RoboFine-VLM Details	23
A.2.1	SFT Data Format	23
A.2.2	Model and Training Details	23
A.2.3	Video Sampling Configuration	24
A.2.4	SFT Prompt Templates	24
A.2.5	Inference and Scalable Annotation	26
A.3	RoboFine-Bench Details	26
A.3.1	Benchmark Construction and Statistics	26
A.3.2	VQA Track Details	26
A.3.3	Caption Track Details	28
A.3.4	Prompt Templates and Evaluation Protocol	29
A.3.5	Judge Robustness	31
A.3.6	Human Alignment Study	31
A.3.7	Caption Cost, Token, and Latency	32
A.3.8	Detailed Benchmark Results	32
A.4	FineVLA-Policy Setup	33
A.4.1	Policy Frameworks	33
A.4.2	Pretraining Datasets and Configuration	33
A.4.3	RoboTwin Fine-Tuning Data and Configuration	34
A.4.4	Instruction Mixing Construction	34
A.4.5	Additional Training Details	34
A.5	RoboTwin Details and Additional Analysis	34
A.5.1	RoboTwin Evaluation Protocol	34
A.5.2	Full RoboTwin Results	35
A.5.3	Mixing-Ratio Analysis	35
A.5.4	Architecture and Scale Analysis	35
A.6	Real-World Policy Details	35
A.6.1	Robot Hardware and Setup	36
A.6.2	Real-World Tasks	36
A.6.3	Real-World Evaluation Protocol	37

A.6.4	Subgoal Definitions for Partial Scoring	37
A.6.5	Per-Factor Language-Critical Scores	37
A.7	Additional Analysis	38
A.8	Reproducibility, Limitations, and Ethics	38
A.8.1	Reproducibility Checklist Support	38
A.8.2	Compute Resources	38
A.8.3	Limitations	38
A.8.4	Societal Impact and Safety	39

This appendix is organized to mirror the logic of the main paper and collects detailed methodology, extended analyses, and reproducibility information that support the claims in Sections 2–5.

A.1 FineVLA-Tool Details

This section provides implementation and annotation details for Section 2. It explains how heterogeneous robot trajectories are converted into a unified action-aligned supervision corpus and how human review is used to maintain annotation quality.

A.1.1 Data Sources and Format Conversion

This subsection supports the data-construction claim in Section 2 by listing the source datasets and the unified-format conversion step used before filtering, clustering, and annotation.

Table 6 summarizes the ten open-source datasets used by FineVLA-Tool before clustering and representative sampling. We convert all trajectories to a unified LeRobot 2.1-style format that standardizes RGB videos, robot states, action sequences, and task metadata across embodiments. This conversion is a prerequisite for consistent filtering, action-state canonicalization, and later cross-dataset annotation.

Table 6: **Source datasets used by FineVLA-Tool.** The table reports the ten datasets retained for fine-grained annotation after selecting the final source list used in this paper.

Dataset	# Trajectories	# Tasks
BridgeData-V2	53,192	19,974
BC-Z	39,350	104
RT-1	87,212	599
Galaxea	113,000	19,627
RoboMIND-V1	73,909	436
RoboMIND-V2	258,786	723
RoboCOIN	104,857	807
RH20T-RoboInter	82,894	147
RDT-1B	6,061	296
DROID-RoboInter	152,986	43,026
Total	972,247	85,739

A.1.2 Action-State Canonicalization

This subsection supports the canonicalization step in Section 2. Its role is to make state and action sequences comparable across datasets that use different temporal conventions and different kinematic parameterizations.

Across datasets, action and state annotations differ in both temporal reference and kinematic representation. We organize these differences along two axes: (i) temporal convention, distinguishing absolute quantities, deltas relative to current state, and offsets relative to the first frame; and (ii) kinematic convention, distinguishing joint-space signals from end-effector-space signals with multiple rotation encodings. We standardize EEf rotations to quaternions in xyzw order.

Table 7: **Canonicalization tokens and their semantics.** Prefixes define temporal reference, while suffixes define the parameterization of robot state or action variables.

Token	Meaning	Notes
abs	Absolute value in a global/world frame	Used by all states
delta	Increment relative to the current state	Action only
rel	Offset relative to the first frame	Action only
joint	Joint / gripper / hand coordinates	Non-EEF modalities
rotvec	Rotation vector (axis-angle)	3D rotation code
quat	Quaternion in xyzw order	Canonical quaternion form
wxyz	Quaternion in wxyz order	Scalar-first order
euler	Euler angles in XYZ order	3D rotation code

For non-EEF variables such as joints, grippers, or hand states, the state is always treated as an absolute quantity. In contrast, the raw action may be stored as an absolute command or a delta command, and is therefore converted into one of `abs_joint`, `delta_joint`, or `rel_joint`. For EEF variables, each pose is represented as 3D position plus a rotation code; the state remains absolute, while the action may use any of the three temporal-reference prefixes.

Table 8: **Canonicalization rules across modality types.** State and action variables admit different canonical type sets for non-EEF and EEF modalities.

Field type	State options	Action options
Non-EEF	<code>abs_joint</code>	<code>abs_joint</code> , <code>delta_joint</code> , <code>rel_joint</code>
EEF (left/right end effector)	<code>abs_rotvec</code> , <code>abs_quat</code> , <code>abs_wxyz</code> , <code>abs_euler</code>	All 12 combinations formed by $\{\text{abs}, \text{delta}, \text{rel}\} \times \{\text{rotvec}, \text{quat}, \text{wxyz}, \text{euler}\}$
Count summary	5 state tags overall	15 action tags overall

A minimal example is as follows. Let $s_t^{\text{joint}} \in \mathbb{R}^d$ be the current joint state and let the raw action be a delta command $\Delta a_t^{\text{joint}}$. The absolute next-state target is

$$\hat{s}_{t+1}^{\text{joint}} = s_t^{\text{joint}} + \Delta a_t^{\text{joint}},$$

while the relative action with respect to the first frame is

$$a_{t+1,\text{rel}}^{\text{joint}} = \hat{s}_{t+1}^{\text{joint}} - s_1^{\text{joint}}.$$

For EEF trajectories, we first convert the raw orientation code to a canonical xyzw quaternion, compose delta poses with the current absolute pose if necessary, and only then derive the desired absolute, delta, or first-frame relative action target.

A.1.3 Quality Filtering and DTW Consistency Check

This subsection supports the cleaning step in Section 2. It explains how we remove invalid videos and trajectories whose actions and states are inconsistent after canonicalization.

We first perform video-level filtering to remove trajectories with invalid or missing videos, extremely short duration, large black-frame segments, or other obvious recording failures. We then apply action-state consistency filtering on canonicalized trajectories. Intuitively, a valid demonstration should exhibit a state evolution that is compatible with the recorded action sequence after both have been converted into a common representation. We therefore measure trajectory-level consistency using DTW and reject samples whose action-state DTW distance exceeds a dataset-specific threshold. This stage removes corrupted logs, mismatched control conventions, and trajectories whose recorded actions do not explain the observed state change.

A.1.4 Action-Based Clustering and Representative Sampling

This subsection provides full implementation details for the representative-sampling step described in Section 2. The goal is to reduce redundancy in large robot corpora while preserving genuinely

distinct execution patterns, so that a fixed annotation budget covers the widest possible range of manipulation strategies.

Pipeline overview. The clustering pipeline proceeds in four stages:

1. **Canonicalization.** All trajectories within a task are converted to their canonical action representation (joint-space or EEf-space with quaternion rotations) following the procedure in Appendix A.1.2.
2. **Pairwise DTW distance computation.** For each pair of trajectories within a task, we compute the DTW distance using a representation-specific frame cost function (defined below).
3. **Hierarchical clustering.** Agglomerative clustering with average linkage is applied to the pairwise distance matrix, and the number of clusters is determined automatically via the largest relative gap in merge heights.
4. **Representative selection.** Two to three high-quality trajectories are selected from each cluster based on proximity to the cluster medoid and trajectory quality metrics (video integrity, action smoothness).

DTW formulation. Open robot datasets are highly redundant: many demonstrations differ only in speed, minor spatial offsets, or camera viewpoint, while expressing the same underlying action pattern. Dynamic Time Warping (DTW) handles temporal misalignment by finding the optimal warping path between two action sequences. Given two sequences $\mathbf{x}_{1:T}$ and $\mathbf{y}_{1:U}$, DTW minimizes the cumulative frame-level distance according to

$$D_{\text{DTW}}(i, j) = c(\mathbf{x}_i, \mathbf{y}_j) + \min\{D_{\text{DTW}}(i-1, j-1), D_{\text{DTW}}(i-1, j), D_{\text{DTW}}(i, j-1)\}.$$

Frame cost function. The frame cost $c(\cdot, \cdot)$ depends on the action-space representation:

- **Joint-space** (`rot_type = none`): All joint values are min-max normalized to $[0, 1]$ per dimension across the task group. The frame cost is

$$c_{\text{joint}}(\mathbf{x}, \mathbf{y}) = w_{\text{pos}} \cdot \|\mathbf{j}_x - \mathbf{j}_y\|_2 + w_{\text{grip}} \cdot |g_x - g_y|,$$

where \mathbf{j} denotes the normalized joint vector and g the gripper state.

- **EEf-space** (quaternion or Euler): The frame cost combines position, rotation, and gripper terms:

$$c_{\text{eef}}(\mathbf{x}, \mathbf{y}) = w_{\text{pos}} \cdot \|\mathbf{p}_x - \mathbf{p}_y\|_2 + w_{\text{rot}} \cdot d_{\text{geo}}(\mathbf{q}_x, \mathbf{q}_y) + w_{\text{grip}} \cdot |g_x - g_y|,$$

where \mathbf{p} is the 3D position, $d_{\text{geo}}(\mathbf{q}_x, \mathbf{q}_y) = 2 \arccos(|\mathbf{q}_x \cdot \mathbf{q}_y|)$ is the quaternion geodesic distance (handling $\mathbf{q} \equiv -\mathbf{q}$), and g is the gripper state. For datasets using Euler angles, orientations are first converted to quaternions.

Default weights are $w_{\text{pos}} = 1.0$, $w_{\text{rot}} = 1.0$, $w_{\text{grip}} = 100.0$. The high gripper weight ensures that gripper open/close transitions—which are critical for distinguishing manipulation strategies—are not overwhelmed by continuous motion differences.

Pairwise distance computation. Since each task typically contains 100–200 trajectories, computing the full $N \times N$ pairwise DTW distance matrix is tractable ($\sim 5\text{k}$ – 20k pairs per task). Each DTW distance is normalized by the warping path length to account for differences in trajectory duration. Computation is parallelized across CPU cores.

Hierarchical clustering and representative selection. We apply agglomerative hierarchical clustering (average linkage) on the DTW distance matrix. The number of clusters k is selected automatically by identifying the largest relative gap in the dendrogram merge heights. We then select two to three representative trajectories per cluster according to cluster size and trajectory quality (proximity to the cluster medoid). Applying this procedure to 972,247 raw demonstrations yields 47,159 representative trajectories for fine-grained annotation. This greatly reduces annotation cost while preserving diversity in manipulation strategy, object interaction, and motion pattern.

Figure 7 shows two task-level clustering examples. In both cases, the DTW distance matrix exhibits clear block structure, and the corresponding MDS embedding separates execution modes that differ in gripper timing, contact duration, or end-effector path. This is the key reason clustering improves annotation efficiency: a single fine-grained instruction can cover multiple redundant demonstrations that share the same execution pattern.

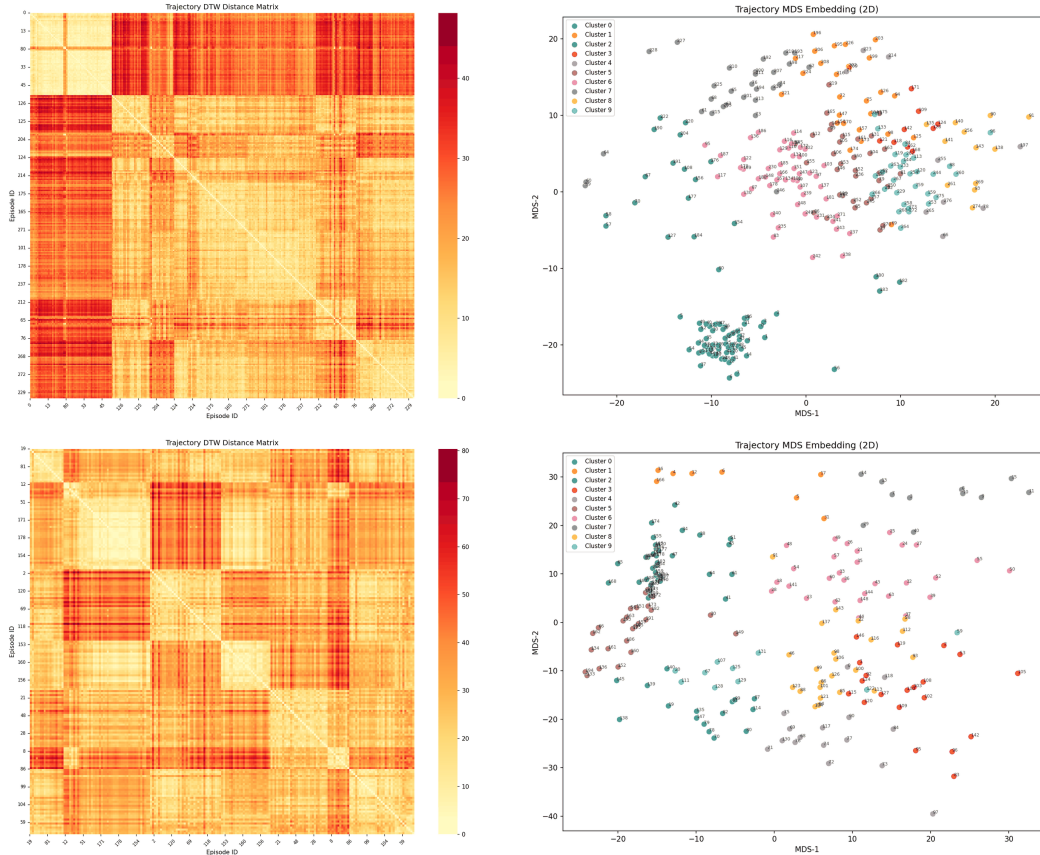


Figure 7: **Qualitative examples of DTW-based trajectory clustering in FineVLA-Tool.** For each task, the left panel shows the pairwise DTW distance matrix and the right panel shows a 2D MDS embedding of the same distances. Clear cluster structure indicates that trajectories with similar manipulation dynamics are grouped together, while differences in gripper timing and end-effector motion patterns are separated into different clusters. This allows one fine-grained instruction to cover multiple redundant demonstrations with the same execution pattern, substantially reducing annotation cost while improving data quality.

A.1.5 Fine-Grained Annotation Schema

This subsection supports the annotation schema referenced throughout the main paper. It defines the ten dimensions used both for data annotation and for benchmark construction.

Table 9: **Fine-grained annotation schema used by FineVLA-Tool.** Each representative trajectory in FineVLA-Data is annotated along ten control-relevant dimensions. The same schema is also used by RoboFine-Bench to construct VQA questions and caption-level atomic facts.

Dimension	What it captures	Typical slots	Examples
Action sequence	The ordered manipulation primitives and gripper states that define the execution process. Captures which actions occur and their temporal order.	Primitive action; gripper state; step order; action transition.	Open gripper → approach mug → grasp handle → lift → place on tray → release.
Active actor	The robot component or body part that performs the action. Important for bimanual manipulation and multi-effector platforms.	Actor identity; left/right hand; both hands; gripper; finger; arm; end-effector.	The right gripper picks up the cup. Both hands lift the container together.
Target object	The object directly manipulated, with visual or spatial attributes to disambiguate among similar objects.	Object category; color; material; shape; size; spatial reference.	The red cup on the left. The small metal spoon inside the bowl.
Initial config.	The pose, state, or spatial relation of the target object before the action begins.	Initial pose; workspace location; attachment state; relational state.	The bottle is standing upright on the table. The drawer is partially open.
Final config.	The pose, state, or spatial relation of the target object after the action is completed.	Final pose; final location; relational state; object state.	The cup ends up on the tray. The drawer is fully closed.
Contact & approach	How the robot approaches the target and where physical contact occurs. Captures control-relevant interaction geometry.	Contact region; approach direction; grasp type; contact modality.	Grasp the mug by the handle from above. Push the drawer from its front panel.
Trajectory & orientation	The translational path, motion direction, path shape, and rotational behavior of the object or end-effector.	Translation direction; path shape; motion extent; rotation direction; rotation angle.	Lift upward. Move to the right along a straight path. Rotate clockwise $\sim 90^\circ$.
Object interaction	Incidental or relational effects on objects other than the target. Captures secondary contacts, collisions, or induced movements.	Interaction type; affected object; contact or collision; relational change.	Placing the book causes the stack to shift. The block brushes against its neighbor.
Failure & recovery	Visible execution failures and recovery behaviors, including retries, slippage, and fail-then-succeed patterns.	Failure type; recovery action; retry behavior; attempt count; slippage.	The robot first fails to grasp, then retries successfully. The object slips before being re-grasped.
Body motion	Motion of the robot base, torso, camera, or other non-end-effector body parts that affects execution.	Base translation; base rotation; torso motion; camera motion.	The mobile base moves forward before the arm reaches the object.

A.1.6 Human-in-the-Loop Verification

This subsection supports the claim that FineVLA-Data is human verified. It summarizes the dimensions checked during review after the initial annotation or model-assisted draft is produced.

Human reviewers compare each step-level description against the corresponding video and verify both semantic correctness and temporal alignment. The review process focuses on the factors most critical for downstream control.

Table 10: **Verification dimensions in the human review stage.** These checks ensure that fine-grained instructions remain temporally aligned and do not introduce hallucinated events.

Verification dimension	What is checked
Temporal order	Whether step order matches the observed execution timeline
Object identity	Whether the manipulated object is correctly identified and disambiguated
Actor identity	Whether the responsible arm / gripper / body part is correctly assigned
Contact region	Whether grasp/contact location and approach side are faithful to the video
Motion direction	Whether translational and rotational directions are described correctly
State transition	Whether initial and final states match the observed change
Hallucinated events	Whether the instruction introduces unsupported actions or recoveries

A.2 RoboFine-VLM Details

This section provides supporting details for the RoboFine-VLM component in Section 2.4. It explains the training data format, the known model setup, and how the resulting model is used as a scalable annotator.

A.2.1 SFT Data Format

This subsection supports the supervised fine-tuning setup described in Section 2.4. Each training sample pairs a robot manipulation video with a prompt asking for a temporally ordered fine-grained action description.

Table 11: **Supervised fine-tuning sample format for RoboFine-VLM.** Each sample maps a robot video to a step-level, action-aligned description derived from FineVLA-Tool annotations.

Field	Description
Input video	Multi-frame robot manipulation video sampled from a trajectory
Prompt	Instruction asking the model to describe the manipulation process step by step
Output target	Temporally ordered fine-grained action description aligned with FineVLA-Tool annotations
Supervision source	Human-verified video-instruction pairs from FineVLA-Data

A.2.2 Model and Training Details

This subsection supports the model description in Section 2.4.

Table 12: **RoboFine-VLM training configuration.**

Item	Value
Base model	Qwen3.5-397B-A17B
Fine-tuning strategy	Full parameter fine-tuning
Training objective	Supervised fine-tuning for step-level robotic action understanding
Training corpus	FineVLA-Tool-generated and human-verified video-instruction pairs
Training sample count	47,159 representative trajectories / video-instruction pairs
Output format	Ordered fine-grained action description
GPUs	256×H200
Global batch size	512
Epochs	9
Training steps	903
Optimizer	AdamW
Learning rate	7e-6, decayed to 7e-7
LR schedule	Linear decay
Wall-clock training time	~40 hours (1 day 16 hours)
Memory per GPU	~105 GB

A.2.3 Video Sampling Configuration

This subsection details how raw robot videos are sampled into frame sequences for SFT. We use two configurations depending on the number of camera views available in each trajectory.

Table 13: **Video sampling configuration for RoboFine-VLM SFT.** Multi-view trajectories concatenate frames from all available cameras, while single-view trajectories allow longer temporal context per video.

Parameter	Multi-view	Single-view
Frame sampling rate	4 fps	4 fps
Max frames per video	512	1024
Max tokens per video	76k	224k

A.2.4 SFT Prompt Templates

This subsection provides the system prompts used during supervised fine-tuning of RoboFine-VLM. We use two prompt variants depending on the number of camera views.

Single-view prompt. The following prompt is used for trajectories with a single camera view:

<p>You are a robot manipulation video annotator.</p> <p>Task: Decompose the video into an ordered sequence of fine-grained steps. Each step must describe exactly one visible physical movement by the robot.</p> <p>For each step, include the following when visually confirmed:</p> <ul style="list-style-type: none"> - action and gripper state (e.g., grasp, pick up, place, push, rotate; open → close, release, maintain grasp) - active actor (left hand, right hand, both hands, gripper, finger) - target object using the task instruction name; disambiguate similar objects by position or appearance (e.g., the red cup on the left, the front-most block) - contact region and approach direction (e.g., by the handle from above, at the top edge from the right) - object initial state or location if relevant (e.g., upright, lying flat, inside the container) - trajectory and orientation change (e.g., move forward, lift up, rotate clockwise/counter-clockwise)

- final placement location and final pose if the object is repositioned
- interaction with other objects (e.g., collision, dragging, tipping, displacement)
- failures, retries, slippage, or fail-then-succeed patterns
- body motion such as base, torso, or camera movement

Rules:

- One step = one physical movement.
- Describe only visible facts. Do not infer hidden actions, intent, or occluded contact.
- Use the robot's egocentric frame: left, right, forward, backward, up, down.
- Keep descriptions short, action-oriented, and literal.
- If a detail is unclear or not visible, omit it.
- Mention dual-arm coordination only when both arms are active; label it as stabilize-and-act, simultaneous, sequential, or handoff.

Output JSON only:

```
{ "Step1": "...", "Step2": "...", "StepN": "..." }
```

Multi-view prompt. The following prompt is used for trajectories with three synchronized camera views (one main view and two wrist views):

You are a robot manipulation video annotator.

Task: Analyze three synchronized views and decompose the robot's behavior into an ordered sequence of atomic physical movements.

View use:

- Main View: primary view for all annotation decisions, including step boundaries, action order, active arm, global motion, object relations, and final results.
- Wrist Views (left/right): auxiliary only. Use them only to refine local details such as gripper state, contact region, approach direction, or slight slip.
- If Wrist Views conflict with the Main View, follow the Main View.

Step requirements:

For each step, include the following when visually confirmed:

- action and gripper state (e.g., grasp, pick up, place, push, rotate; open → close, release, maintain grasp)
- active actor (left hand, right hand, both hands, gripper, finger)
- target object using the task instruction name; disambiguate similar objects by position or appearance (e.g., the red cup on the left, the front-most block)
- contact region and approach direction (e.g., by the handle from above, at the top edge from the right)
- object initial state or location if relevant (e.g., upright, lying flat, inside the container)
- trajectory and orientation change (e.g., move forward, lift up, rotate clockwise/counter-clockwise)
- final placement location and final pose if the object is repositioned
- interaction with other objects (e.g., collision, dragging, tipping, displacement)
- failures, retries, slippage, or fail-then-succeed patterns
- body motion such as base, torso, or camera movement

Rules:

- One step = one physical movement.
- Start a new step when the robot changes primitive action, target, or contact state.
- Describe only visible facts. Do not infer hidden actions, intent, or occluded

```

contact.
- If a detail is unclear or not visually confirmed, omit it.
- Use the robot’s egocentric frame: left, right, forward, backward, up, down.
- Keep descriptions concise, action-oriented, and literal.
- Mention dual-arm coordination only when both arms actively contribute to the
same manipulation event; use stabilize-and-act, simultaneous, or handoff when
applicable.

Output JSON only:
{ "Step1": "...", "Step2": "...", "StepN": "..."}

```

A.2.5 Inference and Scalable Annotation

This subsection supports the scalable-annotation claim in Section 2.4. After fine-tuning, RoboFine-VLM serves both as an evaluation model on RoboFine-Bench and as a scalable annotator for new robot trajectories. Given a video, the model generates a temporally ordered action description in the same semantic space as the FineVLA-Tool annotations. These auto-generated descriptions can then be post-processed and human-verified, allowing fine-grained supervision to be extended beyond the manually reviewed subset without changing the schema.

A.3 RoboFine-Bench Details

This section provides supporting details for RoboFine-Bench, the benchmark component introduced in Section 2.3 and analyzed in Section 4.2. It covers benchmark construction, the VQA and caption tracks, evaluation robustness, and additional result analysis.

A.3.1 Benchmark Construction and Statistics

This subsection supports the benchmark-construction claim in Section 2.3. It summarizes the scale, sampling strategy, and granularity of the benchmark.

Sampling strategy. We sample exactly 50 trajectories from each of the 10 source datasets, yielding 500 benchmark videos in total. This uniform allocation ensures that no single dataset dominates the benchmark and that all 10 data sources contribute equally to the evaluation. The 500 benchmark trajectories are used exclusively for evaluation; RoboFine-Bench contains no training split, and all benchmark videos are disjoint from the RoboFine-VLM SFT training set (see Section 2.3).

Table 14: **Summary statistics of RoboFine-Bench.** The benchmark is built to test fine-grained robotic action understanding rather than only task-level recognition.

Statistic	Value
Videos	500 (50 per dataset × 10 datasets)
Source datasets	10
Robot embodiments	32
Atomic facts	10,816
Avg. annotated steps per sample	4.3
Avg. atomic facts per sample	21.6
VQA questions	1,030

A.3.2 VQA Track Details

This subsection supports the VQA track of Section 2.3. It explains how questions are constructed, how ten annotation dimensions are aggregated into three reporting axes, and how answers are scored.

We construct 1,030 questions that probe execution-level manipulation details across the same ten dimensions used in the annotation schema. The question counts per dimension are given in Table 15. For reporting, these dimensions are aggregated into three higher-level axes: Entity and Scene Grounding, Action and Motion Understanding, and Interaction and State Reasoning.

Table 15: **VQA question distribution across capability dimensions.** This table supports the scale and coverage of the VQA track.

Dimension	# Questions
Action sequence	218
Active actor	52
Body motion	10
Contact and approach	155
Failure and recovery	14
Final configuration	182
Initial configuration	77
Object interaction	26
Target object	85
Trajectory and orientation	211
Total	1030

Table 16: **VQA dimension mapping.** The ten fine-grained annotation dimensions are grouped into three reporting axes for RoboFine-Bench VQA evaluation.

Axis	Abbr.	Constituent dimensions
Entity & Scene Grounding	Gnd.	Active actor, Target object, Initial configuration
Action & Motion Understanding	Act.	Action sequence, Contact & approach, Trajectory & orientation, Body motion
Interaction & State Reasoning	State	Object interaction, Final configuration, Failure & recovery
Overall	—	Average over all ten dimensions

Representative VQA prompts include action recognition, temporal ordering, object grounding, and state-change questions. Examples are shown below:

- **Action Recognition:** “What is the robot doing? (A) Grasping (B) Pushing (C) Lifting (D) Placing”
- **Temporal Ordering:** “Which happens first? (A) Gripper opens (B) Arm moves to cup (C) Cup lifted (D) Cup placed”
- **Object Interaction:** “Which object is the right gripper interacting with? (A) Red block (B) Blue cup (C) Green plate (D) None”
- **State Change:** “State of the drawer after action? (A) Fully open (B) Half open (C) Closed (D) Removed”

Answer scoring is deterministic. Multiple-choice questions are evaluated by option matching; yes/no questions are evaluated by normalized string comparison; and numeric questions are evaluated by value extraction.

VQA question generation prompt. The following prompt is used to generate VQA questions from human-reviewed ground-truth annotations. It operates in two modes: *conflict-based* (when model-generated steps disagree with GT) and *GT-only* (when the two are aligned), ensuring questions target both common errors and diverse fine-grained facts.

```

You are a fine-grained robotics video QA-set builder.

Input: A JSON array. Each sample contains: sample_id, fineGrainedSteps
(model-generated, may contain errors), GT (human-reviewed, always trustworthy).

Task Overview

Two modes of question generation:

Mode A -- Conflict-based QA (when GT and fineGrainedSteps conflict): Generate
questions targeting specific disagreements. The answer must always come from

```

GT. Facts that GT describes but fineGrainedSteps omits: you MAY ask. Facts that fineGrainedSteps describes but GT omits: do NOT ask.

Mode B -- GT-only QA (when GT and fineGrainedSteps are similar): Generate questions purely from GT content. Randomly select 3-5 dimensions from the 13 dimensions below. Do NOT always pick the same dimensions.

For every sample, generate 3-5 QA pairs. At most 3 GT-only (Mode B) questions per sample.

13 Capability Dimensions:

1. action_primitive -- fundamental action type (grasp, push, rotate, etc.)
2. actor_identity -- which arm/hand/gripper performs the action
3. object_recognition -- object category, color, material, shape, size
4. object_disambiguation -- distinguishing similar objects via spatial/attribute cues
5. contact_region -- specific part where gripper contacts the object
6. source_state_or_location -- initial state/position before manipulation
7. trajectory_and_orientation -- direction, path, or rotation during motion
8. placement_specification -- final target location or spatial relation
9. interaction_with_other_objects -- contact/disturbance of non-target objects
10. success_failure_retry -- whether the action succeeds, fails, or retries
11. gripper_state -- open/close/release state at a specific moment
12. temporal_order_and_step_boundary -- ordering of steps and boundaries
13. body_motion -- robot base/torso/camera movement

Dimension Balancing: For Mode B, randomly select dimensions per sample. Do NOT ask two questions on the same dimension within one sample. Across the batch, aim for roughly equal coverage.

Answer Types:

- multiple_choice: 4-8 mutually exclusive options, no "all/none of the above"
- yes_no: answer exactly "yes" or "no"
- number: concise Arabic numeral

Question Writing Rules:

- Each question tests exactly ONE atomic fact
- Must be answerable by watching the video
- Do NOT ask broad questions (e.g., "What does the robot do?")
- Do NOT use visually similar colors as distractors

Output: Valid JSON array only. Each item contains sample_id, status, qas (3-5 items with question_id, mode, capability, answer_type, question, options, answer, reference_text).

A.3.3 Caption Track Details

This subsection supports the caption track of Section 2.3. It defines the two evaluation settings, the atomic-fact representation, and the metrics used to score generated captions.

In the *easy* setting, the original task instruction is provided to the model. In the *hard* setting, the model must infer the manipulation process from visual observations alone. Human-reviewed annotations are converted into atomic facts, and each generated caption is aligned against this fact set using the labels *match*, *partial match*, *contradiction*, *omission*, and *hallucination*. We report three aspect-specific metrics computed from the alignment counts. Let M , P , C , and O denote the number of GT facts labeled as match, partial, contradiction, and omission, respectively. Define $A = M + P + C$ (the number of GT facts addressed by the caption) and $G = M + P + C + O$ (total GT facts). Let H be the number of hallucinated action events and S be the total number of action steps in the generated

caption. The metrics are:

$$\text{Consistency} = \frac{M + 0.5P}{A}, \tag{1}$$

$$\text{Coverage} = \frac{M + 0.5P}{G}, \tag{2}$$

$$\text{Anti-Hallucination} = 1 - \frac{H}{S}, \tag{3}$$

$$\text{Overall} = \frac{\text{Consistency} + \text{Coverage} + \text{Anti-Hallucination}}{3}. \tag{4}$$

Table 17: **Caption-track metric and alignment-label definitions.** This table clarifies how atomic-fact alignment is converted into the reported caption metrics.

Item	Definition
Consistency	Whether the facts stated in the generated caption are correct with respect to the ground truth
Coverage	How much of the ground-truth fact set is recovered by the generated caption
Anti-Hallucination	Whether the caption avoids fabricated actions or states unsupported by the ground truth
Match	Generated fact is correct and aligned to a ground-truth fact
Partial match	Generated fact overlaps with a ground-truth fact but is incomplete or slightly imprecise
Contradiction	Generated fact conflicts with the ground truth
Omission	Ground-truth fact is missing from the generated caption
Hallucination	Generated fact has no support in the ground truth

A.3.4 Prompt Templates and Evaluation Protocol

This subsection provides the exact prompts and evaluation pipelines used for RoboFine-Bench. All evaluated models (Qwen3-VL-Plus, Qwen3.5-Plus, Doubao-Seed-2.0-Pro, Gemini-3.1-Pro, GPT-5.4, and RoboFine-VLM) receive the same visual input format, prompting protocol, and sampling budget within each track.

VQA evaluation pipeline. For each benchmark sample, multi-view video frames are extracted and labeled (e.g., [View: head_rgb], [View: left_wrist_rgb]). All questions for one sample are batched into a single prompt. The model is instructed to return structured JSON answers. Multiple-choice options are randomly shuffled per question (seeded by question ID) to prevent positional bias. Answers are scored deterministically: yes/no questions by normalized string comparison, number questions by value extraction, and multiple-choice questions by option-letter matching.

The VQA system prompt is:

You are an expert robot manipulation video analyst. You will be shown frames from a robot manipulation video with one or more camera views. Each view is labeled (e.g., [View: head_rgb], [View: left_wrist_rgb]). Use information from ALL views to answer the questions. Answer based ONLY on what you observe in the video frames. Be precise and concise.

The VQA user prompt template is:

Watch the video frames carefully and answer ALL of the following questions about this robot manipulation video.

{questions_block}

You MUST return your answers as a JSON object. Use the FULL question_id shown in brackets [] as the key (NOT the short Q1/Q2 label):

```
{"answers": {"<full_question_id>": "<your_answer>", ...}}
```

Rules:

- For yes_no questions: answer EXACTLY "yes" or "no"
- For number questions: answer with JUST a number (e.g. "3")
- For multiple_choice questions: answer with JUST the option letter (e.g. "B")
- Do NOT include explanations in the JSON values -- only the short answer
- You MUST answer ALL questions

Caption evaluation pipeline. The caption track proceeds in two stages:

Stage 1: Caption generation. Given video frames and a prompt asking for temporally ordered step-level action descriptions, each evaluated model generates a manipulation caption. In the easy setting, the original task instruction is provided; in the hard setting, only video frames are given.

Stage 2: LLM-based alignment judging. The generated caption and the pre-extracted ground-truth atomic facts (grouped by capability dimension) are passed to an LLM judge (GPT-5.4-Pro by default). The judge evaluates each GT atomic fact against the raw caption and assigns one of four labels: *match* (caption correctly states the fact), *partial* (caption addresses the event but is materially coarser or incomplete), *contradiction* (caption gives a conflicting value), or *omission* (caption does not mention the fact). Additionally, the judge identifies *hallucinated actions*: action events in the caption that have no correspondence in any GT action_sequence fact.

The alignment judge prompt specifies detailed semantic tolerance policies (color-family equivalence, synonym matching, compatible spatial wording, actor naming equivalence) and strict rules for hallucination detection (only genuinely fabricated actions with no GT basis are flagged). The judge returns a structured JSON with per-fact labels, caption evidence, and aggregate counts. The three reported metrics are then computed from these counts:

- **Consistency:** fraction of caption-addressed GT facts that are match or partial (not contradiction).
- **Coverage:** fraction of GT facts labeled match or partial (not omission).
- **Anti-Hallucination:** penalizes fabricated action events not supported by GT.

The full alignment judge system prompt is provided below:

You are an expert evaluator for fine-grained robot manipulation captions.

You receive:

1. Pre-extracted GT atomic facts (structured, grouped by capability dimension).
2. A raw AI-generated caption (a list of step descriptions, NOT pre-extracted into atomic facts).

Your task is to evaluate each GT atomic fact against the raw caption text and determine:

- For each GT fact: is it match, partial, contradiction, or omission?
- Additionally, identify any hallucinated action events in the caption that do NOT appear in the GT action_sequence facts.

GT Fact Evaluation Rules:

- match: caption clearly states or implies the same information as the GT fact.
- partial: caption addresses the same event but is materially coarser or incomplete.
- contradiction: caption addresses the same event but gives a conflicting value.
- omission: caption does not address this GT fact at all.

Hallucination Detection (action_sequence only):

A hallucinated action must describe a distinct, meaningful action event that no GT action_sequence fact covers, is not a sub-action of a matched GT action, and is not a gripper state change accompanying a matched action.

Output: structured JSON with per-fact labels, caption evidence, and summary counts (match + partial + contradiction + omission == total_gt_facts).

A.3.5 Judge Robustness

This subsection supports the judge-robustness claim made in Section 4.2. It compares caption scores obtained with GPT-5.4-Pro and Gemini-3.1-Pro as alignment judges.

The main-paper caption results use GPT-5.4-Pro as the alignment judge. To test whether the benchmark conclusions are sensitive to the evaluator, we additionally compute a Gemini-3.1-Pro-based counterpart of Table 3. Under Gemini-3.1-Pro, RoboFine-VLM remains the strongest model in both easy and hard settings, and the full model ranking is identical to the GPT-5.4-Pro judge results in both settings. This shows that the benchmark conclusion is robust to the judge model even though absolute scores vary slightly.

Table 18: **Caption benchmark results on RoboFine-Bench (%) under a Gemini-3.1-Pro judge.** We report the same easy/hard caption metrics as in the main paper, but use Gemini-3.1-Pro for caption-fact alignment. **Cons.:** Consistency; **Cov.:** Coverage; **A-Hal.:** Anti-Hallucination. Best value per column is **bold**.

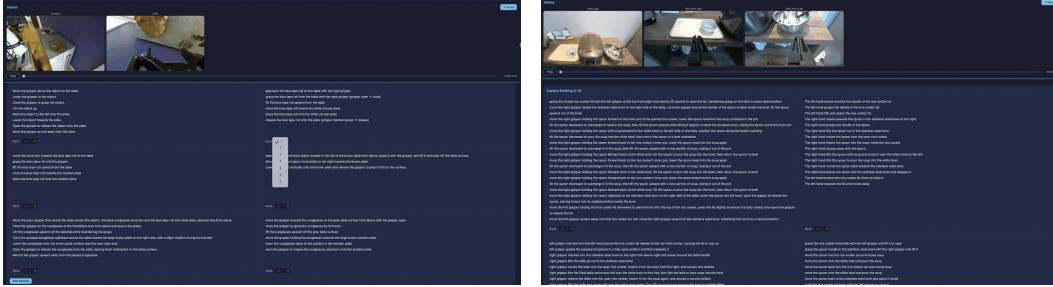
Model	Easy				Hard			
	Overall \uparrow	Cons. \uparrow	Cov. \uparrow	A-Hal. \uparrow	Overall \uparrow	Cons. \uparrow	Cov. \uparrow	A-Hal. \uparrow
Qwen3-VL-Plus	75.1	78.5	56.5	90.2	64.2	72.8	54.1	65.7
Qwen3.5-Plus	77.0	80.4	56.2	94.4	71.6	76.2	52.1	86.6
Doubao-Seed-2.0-Pro	77.1	82.0	56.9	92.5	68.5	75.0	64.8	65.5
Gemini-3.1-Pro	79.3	80.9	70.8	86.1	75.0	79.8	56.4	88.8
GPT-5.4	82.2	82.7	74.2	89.6	78.1	77.8	68.7	87.9
RoboFine-VLM (Ours)	85.2	86.3	75.7	93.7	84.4	84.6	75.7	93.0

A.3.6 Human Alignment Study

This subsection supports the human-alignment claim in Section 4.2. It explains how the 10-human-rater study is constructed and how the benchmark scores are normalized before correlation analysis.

We recruit 10 human raters. For each benchmark sample, annotators are shown the robot video together with six candidate captions, one from each evaluated model: Qwen3-VL-Plus, Qwen3.5-Plus, Doubao-Seed-2.0-Pro, Gemini-3.1-Pro, GPT-5.4, and RoboFine-VLM. Each caption is ranked from 1 to 6, where 1 denotes the best caption and 6 denotes the worst. The protocol is conducted on the same 500 benchmark videos used for automatic caption evaluation.

Annotators jointly consider factual correctness, process coverage, temporal coherence, object grounding, and resistance to hallucination. After annotation, we average the assigned ranks across raters and samples to obtain a single human score per model. These scores are normalized from the theoretical 1–6 range to $[0, 1]$, while benchmark caption Overall scores are normalized from 0–100 to $[0, 1]$. The resulting correlations reported in the main paper are high in both settings: easy Pearson **0.980** and Spearman ρ **1.000**; hard Pearson **0.970** and Spearman ρ **1.000**.



(a) Human ranking interface on a short tabletop manipulation sample. (b) Human ranking interface on a longer multi-step kitchen task.

Figure 8: **Human ranking interface for caption evaluation.** Annotators watch the benchmark video and rank the six candidate captions from best to worst according to fine-grained faithfulness and usefulness. The protocol is designed to validate whether benchmark-induced model ranking is aligned with direct human judgment.

A.3.7 Caption Cost, Token, and Latency

This subsection supports the efficiency discussion in Section 4.2. It reports average token consumption and elapsed time per sample for the caption track.

Table 19 shows that RoboFine-VLM achieves the best caption quality while remaining substantially more token-efficient than several strong closed-source baselines, especially Doubao-Seed-2.0-Pro and Gemini-3.1-Pro.

Table 19: **Caption-track inference cost.** Average total token consumption and average elapsed time per sample on the caption track.

Model	Avg. total tokens	Avg. elapsed (s)
RoboFine-VLM	14,438.1	74.5
GPT-5.4	21,906.6	62.2
Doubao-Seed-2.0-Pro	93,792.2	104.8
Gemini-3.1-Pro	198,271.9	62.8
Qwen3.5-Plus	13,219.8	95.6
Qwen3-VL-Plus	8,352.0	6.4

A.3.8 Detailed Benchmark Results

This subsection supports the concise benchmark discussion in Section 4.2. It provides the more detailed result interpretation moved out of the main paper to save space.

VQA analysis. RoboFine-VLM reaches **71.0%** overall accuracy, outperforming the strongest general-purpose baseline, Gemini-3.1-Pro, by **8.9** absolute points. The largest gain appears on Action and Motion Understanding, where RoboFine-VLM improves from **58.4%** to **68.4%**, indicating a substantial advantage in understanding execution order, contact patterns, and motion dynamics. The gains are also consistent on Entity and Scene Grounding (**72.1%** \rightarrow **78.3%**) and Interaction and State Reasoning (**61.3%** \rightarrow **69.8%**), showing that the benefit of fine-grained supervision extends beyond object recognition to process-level reasoning.

Relative to its base model, Qwen3.5-Plus, supervised fine-tuning on FineVLA-Data raises overall VQA accuracy from **52.6%** to **71.0%**. The improvement is broad-based across all three reporting axes, with gains of **+16.4**, **+17.2**, and **+14.3** points on Gnd., Act., and State, respectively. This comparison isolates the effect of fine-grained action-aligned supervision more directly than cross-model comparison alone, and shows that FineVLA-Data substantially strengthens the robotic video understanding capability of the underlying VLM.

Caption analysis. Instruction input is beneficial for all evaluated models: caption Overall is consistently higher in the easy setting than in the hard setting. The easy-hard gap is especially large

for Qwen3-VL-Plus and Doubao-Seed-2.0-Pro, suggesting that these models rely more heavily on the original task instruction. The same trend appears in Anti-Hallucination: some general-purpose VLMs depend strongly on instruction input to avoid fabricated action content, whereas RoboFine-VLM remains comparatively stable when the instruction is removed.

RoboFine-VLM remains the strongest model overall. In the easy setting, it achieves the best Overall, Consistency, and Coverage scores. In the hard setting, which requires the model to infer the manipulation process directly from video rather than from task-level language priors, RoboFine-VLM is SOTA on all four metrics and improves Overall from the strongest baseline score of **78.1%** to **83.6%**. These results indicate that the gain from fine-grained supervision is not limited to instruction-conditioned captioning, but extends to intrinsic process understanding.

Benchmark validity. Unless otherwise specified, the caption results in Table 3 use GPT-5.4-Pro as the alignment judge. Re-evaluating the same captions with Gemini-3.1-Pro preserves the same model ranking in both easy and hard settings, despite small shifts in absolute scores; the corresponding robustness discussion is reported in Appendix A.3.5. We further compare automatic caption scores with human judgment by asking 10 raters to rank the six models on the same 500 benchmark videos. As shown in Figure 4, the resulting agreement is strong in both settings (easy: Pearson **0.980**, Spearman ρ **1.000**; hard: Pearson **0.970**, Spearman ρ **1.000**), indicating that the caption track is both aligned with human preference and robust to the choice of judge model.

A.4 FineVLA-Policy Setup

This section provides implementation details for the policy setup used in Section 3. It specifies the policy architectures, pretraining configuration, RoboTwin fine-tuning data, and instruction-mixing design used to study the effect of fine-grained language supervision.

Table 20: **Training configurations for FineVLA-Policy.** The table summarizes the backbone, training dataset, optimization length, and compute budget used in the pretraining and RoboTwin fine-tuning stages. The variant names indicate the policy architecture.

Stage	Variant	Backbone	Dataset	Steps	GPUs	Global BS
Pretrain	RDT-OFT	Qwen3.5-4B	RDT	100k	64×A100	512
Pretrain	RDT-GR00T	Qwen3.5-4B	RDT	100k	64×A100	512
Pretrain	AlohaMix-OFT	Qwen3.5-4B	AlohaMix	100k	64×A100	512
RoboTwin SFT	All pretrained variants	Qwen3.5-4B	RoboTwin	100k	8×A100	128

A.4.1 Policy Frameworks

We instantiate FineVLA-Policy with two action-decoding frameworks implemented in the StarVLA codebase. **StarVLA-GR00T** adopts a dual-system design where the VL backbone serves as System 2 for slow reasoning and a DiT-based flow-matching module serves as System 1 for fast action generation, consistent with GR00T N1.5. **StarVLA-OFT** attaches a lightweight MLP head that reads the hidden states of predefined action tokens and regresses continuous actions in parallel with an L1 objective, following OpenVLA-OFT. The two variants share the same Qwen3.5-4B backbone and the same visual observations and language inputs.

A.4.2 Pretraining Datasets and Configuration

We first pretrain three policy variants for 100k steps: **RDT-OFT**, **RDT-GR00T**, and **AlohaMix-OFT**. Here, OFT and GR00T denote the policy architecture, while RDT and AlohaMix denote the training dataset. **AlohaMix** is an ALOHA-only mixture constructed from open-source datasets such as RoboCOIN and RoboMIND, and contains 86,662 episodes across 598 tasks, approximately $13\times$ larger than RDT. All pretraining runs use 64 A100 GPUs for 100k steps, with per-device batch size 8 and global batch size 512.

Table 21 details the composition of AlohaMix. We deliberately restrict the mixture to ALOHA-compatible dual-arm embodiments so that all trajectories share the same kinematic structure. This

single-embodiment design avoids cross-embodiment confounds and lets us attribute performance differences solely to the language supervision signal. Of the 86,662 total episodes, 5,872 have fine-grained annotations produced by FineVLA-Tool and verified by human annotators; these form the FG dataset used in the instruction-mixing experiments (Section 3.2).

Table 21: **AlohaMix pretraining dataset composition.** All sources use ALOHA-compatible dual-arm embodiments. FG annotations denote the number of episodes with human-verified fine-grained instructions from FineVLA-Data.

Source	Tasks	Episodes	Frames	FG Ann.
RDT	296	6,061	3,169,041	1,275
RoboCOIN	81	35,151	23,035,912	2,907
RoboMIND-V1.0	78	9,370	5,891,176	594
RoboMIND-V2.0	143	36,080	74,502,637	1,096
Total	598	86,662	106,598,766	5,872

A.4.3 RoboTwin Fine-Tuning Data and Configuration

We fine-tune the pretrained policies on RoboTwin using the union of the Clean and Random training sets. The resulting supervised fine-tuning corpus contains 27,500 trajectories and 6,075,103 transitions. All RoboTwin fine-tuning runs use 8 A100 GPUs for 100k steps, with per-device batch size 16 and global batch size 128.

A.4.4 Instruction Mixing Construction

For each dataset and architecture, we keep the robot trajectories, action labels, visual observations, and all other training signals fixed; the *only* variable is the language instruction paired with each trajectory. Every trajectory has two instruction variants: a **Raw** goal-level instruction (e.g., the original task name) and a **FG** fine-grained process-level description generated by FineVLA-Tool.

The FG:Raw ratio controls the *sampling probability* during training. For example, FG:Raw = 1:4 means that each trajectory has a $\frac{1}{5}$ probability of being paired with its FG instruction and a $\frac{4}{5}$ probability of being paired with its Raw instruction when sampled for a training step. The trajectory itself, its action labels, and visual observations remain identical regardless of which instruction is drawn. This ensures that observed performance differences are attributable solely to the instruction type.

We compare seven configurations: Raw-only, FG:Raw = 1:4, 1:2, 1:1, 2:1, 4:1, and FG-only. This design isolates the effect of action-aligned language supervision from changes in data scale, embodiment, or action distribution.

A.4.5 Additional Training Details

We use the same backbone, observation interface, and action interface across all instruction-mixing settings within each framework. Real-world training-set construction and optimizer-level hyperparameters will be documented once the final runs are locked.

A.5 RoboTwin Details and Additional Analysis

This section supports the RoboTwin results in Section 4.3. It provides the evaluation protocol, the full mixing-ratio result table, and the compact analyses that explain the inverted-U trend and the interaction with architecture and dataset scale.

A.5.1 RoboTwin Evaluation Protocol

This subsection supports the evaluation setup in Section 4.3. We evaluate policies on the official RoboTwin **Easy** and **Hard** splits and report success rate averaged over 20 episodes per task. A trial is counted as successful only if the task-specific goal condition is completed at the end of the rollout; reported scores are the average success rates on the corresponding split.

A.5.2 Full RoboTwin Results

This subsection provides the complete mixing-ratio table underlying the RoboTwin discussion in the main paper.

Table 22: **Full RoboTwin simulation success rates (%)**. We compare three training settings (RDT-OFT, RDT-GR00T, and AlohaMix-OFT) under seven FG:Raw instruction ratios. Easy/Hard follow the official RoboTwin splits. Best value per column is **bold**.

FG:Raw	RDT-OFT		RDT-GR00T		AlohaMix-OFT	
	Easy↑	Hard↑	Easy↑	Hard↑	Easy↑	Hard↑
Raw-only	61.5	60.0	55.1	53.4	71.8	71.4
FG : Raw = 1 : 4	68.2	66.5	58.2	55.7	75.3	74.3
FG : Raw = 1 : 2	74.1	72.1	61.7	60.9	82.8	78.6
FG : Raw = 1 : 1	73.9	72.4	69.4	68.2	86.8	82.5
FG : Raw = 2 : 1	70.4	68.3	65.9	63.1	80.9	79.3
FG : Raw = 4 : 1	68.6	67.5	64.9	63.2	79.5	78.5
FG-only	62.9	62.0	62.1	61.5	78.3	76.1

A.5.3 Mixing-Ratio Analysis

This subsection supports the mixing-ratio interpretation in Section 4.3. Across all three evaluated settings, success rate first rises and then falls as the FG proportion increases, with a peak around FG : Raw = 1 : 2 to 1 : 1. The trend is therefore consistent with an inverted-U relationship rather than a monotonic preference for either raw-only or FG-only supervision. Empirically, this means that raw instructions primarily specify *what* to achieve, while fine-grained instructions specify *how* to achieve it; the best performance emerges when both signals are present.

A.5.4 Architecture and Scale Analysis

This subsection provides additional analysis on architectural sensitivity and data-scale interaction, complementing the main findings in Section 4.3.

Table 23 summarizes the detailed numbers used in the main-paper discussion. Panel A reports the three representative supervision regimes for each (dataset, framework) setting: Raw-only, the best mixed FG:Raw ratio, and FG-only. Panel B reports the derived comparison gaps used to support the architectural-equalization and data-scale analyses.

Table 23: **RoboTwin analysis summary**. Panel A lists the raw-only, best mixed, and FG-only performance for each setting. Panel B reports the derived gaps used in the architectural and data-scale comparisons. All values are success rates (%).

Panel A: Representative supervision regimes						
Setting	Raw-only	Best mixed ratio	Best mixed	FG-only	Δ (Raw→Best)	Δ (Raw→FG)
RDT-OFT	61.5 / 60.0	1:2 / 1:1	74.1 / 72.4	62.9 / 62.0	+12.6 / +12.4	+1.4 / +2.0
RDT-GR00T	55.1 / 53.4	1:1 / 1:1	69.4 / 68.2	62.1 / 61.5	+14.3 / +14.8	+7.0 / +8.1
AlohaMix-OFT	71.8 / 71.4	1:1 / 1:1	86.8 / 82.5	78.3 / 76.1	+15.0 / +11.1	+6.5 / +4.7

Values are reported as Easy / Hard.

Panel B: Derived comparison gaps				
Comparison	Raw-only gap	Best mixed gap	FG-only gap	Interpretation
OFT – GR00T on RDT	6.4 / 6.6	4.7 / 4.2	0.8 / 0.5	Framework gap narrows as FG ratio increases.
AlohaMix – RDT under OFT	10.3 / 11.4	12.7 / 10.1	15.4 / 14.1	FG benefit is larger at bigger data scale.

A.6 Real-World Policy Details

This section supports the real-world policy experiments in Section 4.4. It records the task definitions and protocol used for the real dual-arm evaluation, while leaving quantitative tables out of the appendix until finalized measurements are available.

A.6.1 Robot Hardware and Setup

This subsection supports the real-world evaluation setting in Section 4.4.

Hardware. We use a Cobot Magic dual-arm robot with three synchronized RGB cameras (two wrist-mounted, one third-person). The action space consists of 14 joint-position commands (7 per arm) and two continuous gripper commands. Policies are trained with action chunks of length 50 and executed asynchronously at inference time. The low-level controller runs at 30 Hz, and inference is served remotely on an 8×A800 GPU server.

Training data. We collect 50 teleoperated demonstrations for each of 12 tabletop tasks (600 episodes total). All demonstrations are recorded with joint-space actions at 30 Hz and synchronized multi-view video. We train a single language-conditioned policy starting from the pretrained checkpoint (Section 3) and fine-tune for 100k steps on 8 GPUs (global batch size 4, ~1.5 days wall-clock time).

Inference. At test time, the policy receives three RGB frames (one per camera) and a language instruction, and outputs an action chunk of 50 steps. Actions are dispatched asynchronously to the low-level controller. No post-processing or action filtering is applied.

A.6.2 Real-World Tasks

This subsection supports the task selection described in Section 4.4. The real-world evaluation suite contains two general manipulation tasks, five in-distribution instruction-sensitive task families (each comprising a paired variant), and one out-of-distribution compositional probe, each probing a specific control factor: *Clean Table* and *Stack Block* (routine manipulation), *Color* (object color grounding), *Pose* (initial-state grounding), *Approach* (approach direction), *Rotate* (rotation direction), *Arm* (active-arm selection, $R \rightarrow R / L \rightarrow L$), and *Arm+Target* (active-arm selection with unseen actor-target binding, OOD probe). Table 24 lists the paired variants and their corresponding language instructions.

Table 24: **Real-world evaluation tasks and paired variants.** Each instruction-sensitive factor is tested with two complementary language variants under the same visual scene. [†] L → R uses an unseen actor-target binding (OOD probe).

Factor	Instruction A	Instruction B	Type
Clean Table	Clean up the table.	—	General
Stack Block	Stack the blue block on top of the red block.	—	General
Color	Put the red pen into the pen cup.	Put the blue pen into the pen cup.	ID
Pose	Pick up the cup lying on the table and place it into the box.	Pick up the cup standing on the table and place it into the box.	ID
Approach	Grasp the block from above, move it over the pink bowl, and release it.	Grasp the block from the right side, move it over the pink bowl, and release it.	ID
Rotate	Rotate the pen clockwise for 90 degrees.	Rotate the pen counter-clockwise for 90 degrees.	ID
Arm	Right hand pick up the block and place it into the right bowl.	Left hand pick up the block and place it into the left bowl.	ID
Arm+Target [†]	Right hand pick up the block and place it into the right bowl.	Left hand pick up the block and place it into the right bowl.	OOD

A.6.3 Real-World Evaluation Protocol

This subsection supports the real-world partial-score numbers reported in the main paper. Each task is evaluated over 10 trials. A trial is scored by manually checking ordered subgoals; a completed subgoal receives proportional credit. Between trials, the scene is reset to the designated initial configuration before the next evaluation begins.

A.6.4 Subgoal Definitions for Partial Scoring

Each task is decomposed into ordered subgoals. A trial receives credit proportional to the fraction of completed subgoals. Table 25 lists the subgoal sequence for each task. The **language-critical subgoal** (marked with \star) is the one whose completion requires resolving the fine-grained instruction factor.

Table 25: **Subgoal definitions for real-world partial scoring.** \star marks the language-critical subgoal for each task.

Task	Ordered Subgoals
Clean Table	Reach → Grasp → Lift → Place in bin
Stack Block	\star Identify target block → Reach → Grasp → Transport → Align & Stack
Red Pen	\star Identify correct color → Reach → Grasp → Lift
Lying Pen	\star Identify pose → Approach from correct angle → Grasp → Lift
R → R	\star Select right arm → Reach → Grasp → Transport → Place in right bowl
L → R (OOD)	\star Select left arm → Reach → Grasp → Transport → Place in right bowl
Grasp Above	\star Approach from above → Grasp → Lift
Rotate \odot	Grasp → \star Rotate clockwise 90° → Release

A.6.5 Per-Factor Language-Critical Scores

This section provides the raw trial counts (out of 10) underlying the language-critical accuracy percentages reported in the main text. Table 26 reports, for each control factor, the number of trials in which the language-critical subgoal was satisfied.

The language-critical scores confirm the inverted-U trend observed in the overall partial scores: the 1:1 mixed setting achieves the best controllability on in-domain factors. Notably, the higher-FG variants (2:1 and 4:1) achieve the highest OOD arm-selection scores, indicating that dense process-level supervision strengthens sensitivity to the arm factor—which is well-covered in training—even for unseen actor-target combinations. However, this improved arm selection does not translate into task completion because the target-bowl binding remains unresolved.

Table 26: **Language-critical subgoal success rate** (out of 10 trials) per control factor. Higher values indicate better language-conditioned controllability independent of downstream execution quality.

Supervision	Target Spec.	Color Ground.	Pose Ground.	Arm Select.	Approach Dir.	Rotation Dir.	Arm (OOD)
Raw-only	7	5	4	8	7	9	3
FG:Raw = 1:4	7	6	5	8	7	9	3
FG:Raw = 1:2	8	7	7	9	8	9	6
FG:Raw = 1:1	9	8	8	9	9	10	6
FG:Raw = 2:1	8	7	7	9	8	9	4
FG:Raw = 4:1	7	6	6	9	8	9	4
FG-only	7	5	7	8	8	9	5

A.7 Additional Analysis

This section collects supplementary observations from the RoboTwin experiments that are useful for interpretation but not required for the main narrative.

FG supervision narrows the architecture gap. Comparing StarVLA-OFT and StarVLA-GR00T on the same dataset (RDT), OFT is clearly stronger under Raw-only supervision (gap of 6.4/6.6 on Easy/Hard), but the gap shrinks as FG ratio increases and nearly vanishes under FG-only (0.8/0.5). This suggests that dense language supervision alleviates a supervision bottleneck, reducing the policy’s dependence on decoder architecture choice.

FG supervision benefits more from larger data scale. Comparing RDT-OFT and AlohaMix-OFT, the gain from FG supervision is larger on the bigger AlohaMix dataset. The FG-only improvement over Raw-only grows from +1.4/+2.0 (RDT) to +6.5/+4.7 (AlohaMix). As trajectory diversity grows, dense action-aligned language has more distinct patterns to bind to, suggesting that FG supervision should become even more valuable at larger training scale.

Detailed per-setting numbers supporting both observations are reported in Table 23.

A.8 Reproducibility, Limitations, and Ethics

This section supports the reproducibility, limitation, and ethics-related claims referenced by the NeurIPS checklist. It summarizes the compute budget used in the main training experiments, clarifies the current limitations of the pipeline, and records the intended release scope.

A.8.1 Reproducibility Checklist Support

The main paper and appendix together document the data-construction pipeline, benchmark protocol, policy architectures, instruction-mixing setup, and the training configurations used in the experiments. In particular, Appendix A.1 details the construction of FineVLA-Tool, Appendix A.3 details RoboFine-Bench, and Appendix A.4 details the policy-training setup used in RoboTwin.

A.8.2 Compute Resources

RoboFine-VLM supervised fine-tuning is performed for 903 steps on 256 NVIDIA H200 GPUs with global batch size 512, learning rate decayed from $7e-6$ to $7e-7$, taking approximately 40 hours and using roughly 105 GB of memory per GPU. Policy pretraining is performed for 100k steps on 64 A100 GPUs with global batch size 512, taking approximately 48 hours per run and using roughly 70 GB of memory per GPU. RoboTwin fine-tuning is performed for 100k steps on 8 A100 GPUs with global batch size 128, taking approximately 48 hours per run and using roughly 75 GB of memory per GPU.

A.8.3 Limitations

The current work has two main limitations. First, although RoboFine-VLM provides high-quality scalable annotation, a small portion of generated annotations still requires manual verification, so the pipeline does not fully eliminate human-in-the-loop supervision. Second, while the method is

validated on multiple datasets, RoboTwin, and a set of real-world tasks, broader validation across additional robot embodiments and a larger set of real-world tasks remains future work.

A.8.4 Societal Impact and Safety

Fine-grained language supervision can improve the controllability and transparency of robot behavior by making execution constraints more explicit. At the same time, deployment on real robotic systems still requires external safety constraints, because incorrect grounding, hallucinated action details, or control failures may lead to unintended physical interactions.